THE JOURNAL OF BIOLOGICAL CHEMISTRY VOL. 290, NO. 13, pp. 8331–8347, March 27, 2015

Roles of mRNA Fate Modulators Dhh1 and Pat1 in TNRC6-dependent Gene Silencing Recapitulated in Yeast*

Received for publication, September 28, 2014, and in revised form, January 13, 2015 Published, JBC Papers in Press, February 5, 2015, DOI 10.1074/jbc.M114.615088

Shiho Makino[‡1], **Yuichiro Mishima**[§¶2], **Kunio Inoue**[‖], **and Toshifumi Inada**[‡3]

From the [‡]*Graduate School of Pharmaceutical Sciences, Tohoku University, Sendai 980-8578, Japan, the* [§]*Institute of Molecular and Cellular Biosciences and the* [¶]*Department of Medical Genome Sciences, University of Tokyo, Bunkyo-ku, Tokyo 113-0032, Japan, and the* [‖]*Graduate School of Science, Kobe University, Kobe 657-8501, Japan*

Background: Animal microRNAs silence their target mRNAs by promoting mRNA degradation and inhibiting translation via GW182/TNRC6.
Results: TNRC6 induces silencing effects in *S. cerevisiae* via CCR4-NOT complex and Dhh1-Pat1 when tethered to reporter mRNAs.
Conclusion: TNRC6 utilizes the conserved mRNA fate modulators for gene silencing in yeast.
Significance: Yeast genetic tools are now available to study intricate actions of TNRC6.

The CCR4-NOT complex, the major deadenylase in eukaryotes, plays crucial roles in gene expression at the levels of transcription, mRNA decay, and protein degradation. GW182/TNRC6 proteins, which are core components of the microRNA-induced silencing complex in animals, stimulate deadenylation and repress translation via recruitment of the CCR4-NOT complex. Here we report a heterologous experimental system that recapitulates the recruitment of CCR4-NOT complex by TNRC6 in *S. cerevisiae*. Using this system, we characterize conserved functions of the CCR4-NOT complex. The complex stimulates degradation of mRNA from the 5′ end by Xrn1, in a manner independent of both translation and deadenylation. This degradation pathway is probably conserved in miRNA-mediated gene silencing in zebrafish. Furthermore, the mRNA fate modulators Dhh1 and Pat1 redundantly stimulate mRNA decay, but both factors are required for poly(A) tail-independent translation repression by tethered TNRC6A. Our tethering-based reconstitution system reveals that the conserved architecture of Not1/CNOT1 provides a binding surface for TNRC6, thereby connecting microRNA-induced silencing complex to the decapping machinery as well as the translation apparatus.

The CCR4-NOT complex is a multisubunit complex involved in many aspects of mRNA metabolism (1–3). Its conserved functions include deadenylation catalyzed by the two deadenylase subunits CAF1/POP2 (CNOT7/8 in vertebrates) and CCR4 (CNOT6 in vertebrates). These two enzymes are incorporated into the complex via a direct interaction between CAF1 and the scaffold protein CNOT1 (4, 5). Thus, recruitment of the CCR4-NOT complex to mRNAs promotes deadenylation, which is usually followed by decapping and 5′-to-3′ degradation by Xrn1 (6, 7). In addition, recent studies have shown that the CCR4-NOT complex provides a link to the decapping machinery. For example, in *Saccharomyces cerevisiae*, the CCR4-NOT complex associates with Dhh1, a decapping activator (8). Similarly, in *Drosophila* and mammals, the CCR4-NOT complex interacts with the Dhh1 homolog Me31B/DDX6/RCK1/p54 and the Pat1 homolog HPat/PatL1 (9–12). HPat/PatL1 in turn associates with the decapping enzyme Dcp2 and its activators Dcp1 and Edc3, thereby organizing assembly of the decapping machinery (9, 13, 14). Moreover, Dhh1 and Pat1 also function in translation repression. In *S. cerevisiae*, Dhh1 or Pat1 is required for translation repression under glucose deprivation, and both Dhh1 and Pat1 repress translation initiation *in vitro* (15). *Drosophila* Me31B and vertebrate DDX6 also act as translation repressors (11, 12, 16–19). These observations imply that the CCR4-NOT complex coordinates multiple processes of mRNA degradation and translation repression rather than merely promoting deadenylation.

MicroRNAs (miRNAs)[4] are small non-coding RNAs that negatively regulate gene expression by inducing translational repression, mRNA degradation, and deadenylation (20–29). miRNAs regulate their target mRNAs by associating with specific protein factors to form the miRNA-induced silencing complex (miRISC). Argonaute (Ago), a core component of miRISC, directly incorporates miRNAs (30). *Drosophila* GW182 and its vertebrate ortholog TNRC6A-C (trinucleotide repeat-containing 6 A-C) interact with Ago via their N-terminal glycine and tryptophan (GW) repeats, whereas their C-terminal silencing domains provide a platform for interactions with RNA reg-

* This study was supported by Grant-in-aid for Scientific Research on Innovative Areas "RNA regulation" (20112006) and "Nascent chain biology" (26116003) (to T. I.) and "non-coding RNA" (24115711) (to Y. M.) from the Ministry of Education, Culture, Sports, Science, and Technology of Japan and by Research Grants in the Natural Sciences, Mitsubishi Foundation (to T. I.).

[1] Recipient of a Japan Society for the Promotion of Science Research Fellowship.
[2] To whom correspondence may be addressed: Dept. of Medical Genome Sciences, University of Tokyo, Bunkyo-ku, Tokyo 113-0032, Japan. Tel.: 81-3-5841-7894; Fax: 81-3-5841-8485; E-mail: mishima@iam.u-tokyo.ac.jp.
[3] To whom correspondence may be addressed: Graduate School of Pharmaceutical Sciences, Tohoku University, Sendai 980-8578, Japan. Tel.: 81-22-795-6874; Fax: 81-22-795-6873; E-mail: tinada@m.tohoku.ac.jp.

[4] The abbreviations used are: miRNA, microRNA; DIG, digoxigenin; qRT-PCR and qPCR, quantitative RT-PCR and PCR, respectively; MO, morpholino oligomer; miRISC, miRNA-induced silencing complex; PABP, poly(A)-binding protein; cRACE, circularized rapid amplification of cDNA ends; DN, dominant negative.

TABLE 1
Yeast strains and plasmids used in this study

Strain/Plasmids	Genotype/plasmid	Source
Strains		
W303-1a	*MATa ade2 his3 leu2 trp1 ura3 can1*	Laboratory stock
YIT2007	W303-1a *xrn1Δ::kanMX*	Ref. 49
YIT2013	W303-1a *ski2Δ::kanMX*	Ref. 67
YIT2030	W303-1a *pat1Δ::natMX*	This study
YIT2031	W303-1a *dhh1Δ::kanMX*	This study
YIT2032	W303-1a *pat1Δ::natMX4, dhh1Δ::kanMX4*	This study
YIT2033	W303-1a *ccr4Δ::kanMX*	This study
YIT2034	W303-1a *caf1Δ::kanMX*	This study
Plasmids		
pIT2068	p*GAL1p-AUG-FLAG-MPT4ΔN-PGK1 (3′ UTR) URA3 CEN*	Ref. 49
pIT2069	p*GAL1p-AUG-FLAG-MPT4ΔN-PGK1 (3′ UTR)-MS2 URA3 CEN*	Ref. 49
pIT2070	p*GAL1p-No-AUG-FLAG-MPT4ΔN-PGK1 (3′ UTR) URA3 CEN*	Ref. 49
pIT2071	p*GAL1p-No-AUG-FLAG-MPT4ΔN-PGK1 (3′ UTR)-MS2 URA3 CEN*	Ref. 49
pIT2082	p*GAL1p-No-AUG-FLAG-MPT4ΔN-PGK1 (3′ UTR)-Rz URA3 CEN*	Ref. 49
pIT2083	p*GAL1p-No-AUG-FLAG-MPT4ΔN-PGK1 (3′ UTR)-MS2-Rz URA3 CEN*	Ref. 49
pIT2139	p*GAL1p-AUG-FLAG-MPT4ΔN-PGK1 (3′ UTR)-MS2-Rz URA3 CEN*	This study
pIT2140	p*GAL1p-AUG-FLAG-MPT4ΔN-PGK1 (3′ UTR)-Rz URA3 CEN*	This study
pIT2141	p*TEF1p-FLAG-MS2 LEU2 CEN*	This study
pIT2142	p*TEF1p-FLAG-MS2-zTNRC6AMid LEU2 CEN*	This study
pIT2143	p*GPD1p-Dhh1-HA URA3 CEN*	This study
pIT2144	p*GPD1p-Pat1-HA URA3 CEN*	This study
pIT2145	p*GPD1p-Not1-HA URA3 CEN*	This study
pIT2146	p*TEF1p-FLAG-MS2-dmGW182Mid LEU2 CEN*	This study
pIT2147	p*GPD1p-Dhh1-FLAG LEU2 CEN*	This study
pIT2148	p*GPD1p-Dhh1 LEU2 CEN*	This study
pIT2149	p*GAL1p-GFP-MS2 URA3 CEN*	This study
pIT2150	p*GAL1p-GFP-MS2-Rz URA3 CEN*	This study
pIT2151	p*GAL11p-GFP URA3 CEN*	This study
pIT2152	p*GAL1p-GFP-Rz URA3 CEN*	This study
pIT2155	p*TEF1p-FLAG-MS2-zTNRC6AMid mutants QSR and W LEU2 CEN*	This study
M44	p*CS2 + HA-λN-zTNRC6A-Mid-globin3′ UTR*	Ref. 40
M277	p*CS2 + HA-λN-MS2-globin 3′ UTR*	This study
M338	p*CS2 + MT-CNOT7-D40A,E42E,C67E,L71E-sv40*	This study
M342	p*CS2 + MT-DCP2-E147A,E148A-sv40*	This study

ulatory factors, including poly(A)-binding protein (PABP), PAN3 of the PAN2-3 deadenylase complex, and CNOT1 (25, 31–36). The CCR4-NOT complex, which is recruited to mRNAs by miRISC, promotes deadenylation via the activities of CAF1 and CCR4 (25, 37). miRISC might further accelerate mRNA decay by recruiting decapping factors in a manner that is independent of their effects on deadenylation (38). In addition, the CCR4-NOT complex may play a role in miRNA-mediated translation repression (34, 35). miRNA can induce translation repression independent of deadenylation (39–41), and the CCR4-NOT complex does so in tethering experiments (34, 42). The interaction of a MIF4G domain of human CNOT1 with DDX6, through a structural arrangement that is analogous to the MIF4G domain of eIF4G and eIF4AI, contributes to the miRNA-mediated silencing (11, 12, 43). These observations indicate that miRISC achieves post-transcriptional silencing via conserved but intricate functions of the CCR4-NOT complex.

S. cerevisiae lacks the small RNA-producing enzyme Dicer and Ago and therefore does not produce canonical siRNAs and miRNAs. However, the basic machinery for controlling mRNA stability and translation, including the CCR4-NOT complex, decapping factors, and translation initiation factors, is highly conserved (6, 7). Notably, the yeast Pumilio-like protein Puf5/Mpt5 binds to the CCR4-NOT complex to silence and deadenylate specific mRNAs (44, 45), suggesting that the CCR4-NOT complex is involved in sequence-specific post-transcriptional regulation independent of the emergence of miRNAs. Previously, the Bartel and Roth laboratories (46, 47) showed that gene silencing by siRNA could be reconstituted in *S. cerevisiae* by expressing either *Saccharomyces castellii* Ago1 and Dicer1 or human Ago2, Dicer, and TRBP.

In this study, we successfully recapitulated two hallmarks of animal miRISC-mediated silencing in *S. cerevisiae* by tethering the middle domain of zebrafish TNRC6A to reporter mRNAs. Using mutant yeast strains, we showed that zebrafish TNRC6A directly stimulates decapping and 5′-to-3′ mRNA decay in a Not1-dependent but poly(A) tail- and translation-independent manner. In addition, we showed that the Dhh1 and Pat1 play crucial roles not only in stimulation of mRNA decapping but also in translational repression. These results indicate that the conserved architecture of Not1/CNOT1 provides a binding surface for TNRC6, thereby connecting miRISC to the decapping machinery and translation apparatus. Furthermore, miR-430-mediated mRNA decay was differentially susceptible to inhibition of deadenylation in zebrafish embryos. This tethering-based reconstitution system in yeast will complement miRNA studies in animal cells, in which genetic approaches are sometimes not applicable.

EXPERIMENTAL PROCEDURES

Strains and Other Methods—Yeast strains and plasmids are listed in Table 1. Information about the oligonucleotides used for poly(A) tail analysis and qRT-PCR are listed in Table 2. Polysome analysis was performed as described (48).

Determination of mRNA Stability—Yeast cells were grown in minimal medium containing 2% galactose. Cells were grown to $A_{600} = 0.6$ and harvested and resuspended in medium contain-

TABLE 2
The oligonucleotides used for poly(A) tail analysis and qRT-PCR

Name/Description	Sequence
PAT reverse	5′-GGTAATACGACTCACTATAGCGAGACCCCCCCCCCTT-3′
eif4ebp2 PAT forward	5′-CAAACTATCAGAAATGCATTTAGTTCTG-3′
gstm PAT forward	5′-TCAGGTGAGTGTTGCATTTTG-3′
acadl PAT forward	5′-ATCATATGGTCTACGCCGAGAG-3′
gfp forward	5′-AAGGGCATCGACTTCAAGGAG-3′
gfp reverse	5′-GATGCCGTTCTTCTGCTTGTC-3′
fluc qPCR forward	5′-AGAACTGCCTGCGTGAGATTC-3′
fluc qPCR reverse	5′-ACCGTGATGGAATGGAACAAC-3′
act1b qPCR forward	5′-TTGTTGGACGACCCAGACATC-3′
act1b qPCR reverse	5′-ATGGGGTATTTGAGGGTCAGG-3′
eif4ebp2 qPCR forward	5′-ACGACTCAACGCAGCTACCTC-3′
eif4ebp2 qPCR reverse	5′-CGGTCCAACAGGAACTTACGA-3′
gstm qPCR forward	5′-GCTCCTGCACCTCATTTTGAAG-3′
gstm qPCR reverse	5′-ACCGGTGTATTCCAACAGCAG-3′
acadl qPCR forward	5′-CTATGTGATGCAGCGGAAGG-3′
acadl qPCR reverse	5′-TGAATGCCCGACCTACACAG-3′

ing 2% glucose to inhibit transcription from the *GAL1* promoter. At the times indicated, the cells were harvested to prepare RNA samples using hot phenol. The mRNA levels of reporter genes were determined by Northern blotting using digoxigenin (DIG) reagents. Non-radioactive probes were prepared by PCR-based nucleic acid labeling using commercial kits. Hybridization probes were detected according to the procedure specified by the manufacturer (Roche Applied Science). The DIG-labeled probes were prepared with the following oligonucleotides: GFP (5′- GCTCTAGAATGAGTAAAGGAGAAGAACTTTTCAC-3′ and 5′- GGACTAGTTTTGTATAGTTCATCCATGCCA-3′) and 3-phosphoglycerate kinase 1 (PGK1) 3′-UTR (5′- GGGAATTTAAATTGAATTGAATTGAAATCGATAG-3′ and 5′-GGGAATTCCGATTGACCAATATATGTCTCTGAATGCC-3′). The intensity of the bands on the blots was quantified using the LAS4000 and Multi-Gauge version 3.0 (Fuji Film). Relative RNA levels were determined by comparison with a standard curve prepared with a series of dilutions of time 0 samples (just before the addition of glucose).

Western Blotting—Yeast cells were grown in minimal medium containing 2% galactose. When the culture reached an A_{600} of 0.6, the cells were harvested. The protein products of FLAG-tagged reporter genes were detected by Western blotting using an anti-FLAG antibody (F1804, Sigma) and a horseradish peroxidase-conjugated secondary antibody (GE Healthcare). The intensity of the bands on the blots was quantified using a LAS4000 imager and Multi-Gauge version 3.0 (Fuji Film). The relative level of the protein product was determined by comparison with a standard curve prepared with a series of dilutions. Western blotting with zebrafish embryos was performed as described previously (40).

Immunoprecipitation—Yeast cells were grown in minimal medium containing 2% glucose. When the culture reached an A_{600} of 0.8, the cells were harvested. Cell extracts were prepared with lysis buffer (20 mM Tris-HCl, pH 7.4, 100 mM KCl, 2 mM $MgCl_2$, 2 mM DTT, 0.5 mM PMSF) by inversion with beads. Cell extracts were incubated with anti-FLAG M2 resin in IXA-150 buffer (50 mM Tris-HCl, pH 7.5, 150 mM KCl, 12 mM $Mg(OAc)_2$, 1 mM DTT, 1 mM PMSF) and then washed four times and eluted with 0.5 mg/ml FLAG peptide.

Measuring the Presence of mRNA Cap Structure—20 μg of RNA samples were incubated in the absence or presence of 10 units of tobacco acid pyrophosphatase (Epicenter) at 37 °C for 90 min. After phenol extraction and ethanol precipitation, RNA samples were divided into two groups and incubated in the absence or presence of 1 unit of Terminator 5′-phosphate dependent exonuclease (Epicenter) at 30 °C for 45 min. 100 ng of *in vitro*-transcribed 5′-triphosphate GFP RNA was added to the reaction to confirm substrate specificity of Terminator exonuclease.

Pulse-labeling Experiments—Yeast cells were grown exponentially at 30 °C in minimal media lacking methionine and cysteine. A 10-ml aliquot of yeast cells was labeled with 100 μCi of [^{35}S]methionine and cysteine (NEG072, PerkinElmer Life Sciences) for 10 min. This was followed by the addition of cold amino acids, to a final concentration of 40 mg/ml. The cells were then collected, and cell extracts were prepared using Y-PER (yeast protein extraction reagent) (Thermo Scientific). Cell extracts were incubated with a GFP antibody (Santa Cruz Biotechnology, Inc.) and protein G-agarose (Roche Applied Science) in IXA-100 buffer (48). The antibody-bound agarose was then washed three times. Immunoprecipitated samples were separated by SDS-polyacrylamide gel electrophoresis. The radioactivity of the precipitated proteins was measured using a Typhoon FLA 9000 imager (GE Healthcare).

Plasmid Construction—A reporter plasmid, p*GAL1p-FLAG-MPT4ΔN-PGK1* (3′-UTR) was described previously (49). To construct pIT2149–2152, *MPT4ΔN* was replaced by GFP ORF using XbaI and BamHI sites in p*GAL1p-FLAG-MPT4ΔN-PGK1* (3′-UTR).

To construct pIT2141 (p*TEF1p-FLAG-MS2*), a DNA fragment encoding *FLAG-MS2* coat protein was amplified by PCR from p*TEF1p-FLAG-MS2* (49) using the primers OIT1822 (5′-TAGATGTCTAGAATGGACTACAAGGACGACGATGACAAGGCT-3′) and OIT1948 (5′-TTGAACGGATCCGTAGATGCCGGAGTTTGCTGCG-3′) and inserted between XbaI and BamHI sites in p*TEF1p* (50). To construct pIT2142 (p*TEF1p-FLAG-MS2-zebrafish TNRC6A Mid*), a DNA fragment encoding the middle domain (residues 1310–1567) of zebrafish TNRC6A was amplified by PCR from p*CS2-HA-lambdaN-zebrafish TNRC6A* (40) using the primers OIT1824 (5′-TAGATGGGATCCGGAGTTCCCTGAGCTCGTTCAGTAATTTCCCT-3′) and OIT1825 (5′-TTGAACCTCGAGTCAAGAGCTGCCCCAGCCTGCCAGT-3′) and inserted be-

tween BamHI and XhoI sites in p*TEF1p-FLAG-MS2*. To construct pIT2155 (p*TEF1p-FLAG-MS2-zebrafish TNRC6A Mid mutants QSR and W*, which contains mutations that disrupt the interaction between CNOT1 and GW182/TNRC6 in human and *Drosophila* cells (33, 34), a DNA fragment encoding the zebrafish TNRC6A Mid domain in which Gln-Ser-Arg and Trp residues were substituted to alanines (Gln-1343, Ser-1344, Arg-1345, Trp-1349, Trp-1404, Trp-1419, Trp-1429, Trp-1484, Trp-1512, Trp-1527, Trp-1555, Trp-1565) was chemically synthesized and cloned between BamHI and XhoI sites in p*TEF1p-FLAG-MS2*. To construct pIT2146 (p*TEF1p-FLAG-MS2-dmGW182 Mid*), a DNA fragment encoding the middle domain (residues 861–1116) of dmGW182 was amplified by PCR from p*Ac5.1B-lambdaN-HA-DmGW182* (51) using the primers OIT2469 (5′-TAGATGCCCGGGCAAGGAGCGTCCAATCAACAATCCCGATTA-3′) and OIT2443 (5′-TTGAACGTCGACTCAGGAGCCCCAAGTGGTGTTACCACCTGTCCA-3′) and inserted between SmaI and XhoI (compatible end of SalI) sites in p*TEF1p-FLAG-MS2* in which an *MS2* tag was inserted between XbaI and SmaI sites. To construct pIT2143 (p*GPD1-DHH1-HA*), pIT2147 (p*GPDp-DHH1-FLAG*), and pIT2148 (p*GPDp-DHH1*), *DHH1* ORF was amplified from the *S. cerevisiae* genome using the forward primer OIT2398 (5′-TAGATGGGATCCATGGGTTCCATCAATAATAACTTCAACA-3′), and reverse primers are as follows: *DHH1-HA*, OIT2399 (5′- TTGAACGTCGACTTACGCGTAGTCTGGGACGTCGTATGGGTAATACTGGGGTTGTGACTGACCAGGTGGC-3′); *DHH1-FLAG*, OIT2659 (5′-TTGAACGTCGACTTACTTGTCGTCGTCGTCCTTGTAGTCATACTGGGGTTGTGACTGACCAGGTGGC-3′); *DHH1-nontag*, OIT1952 (5′- TTGAACGTCGACTTAATACTGGGGTTGTGACTGACCAGGTGG-3′). Subsequently, these DNA fragments were inserted between BamHI and SalI sites in p*GPD1p* and p*GPDp*. To construct pIT2144 (p*GPDp-PAT1-HA*), the *PAT1* gene was amplified from *S. cerevisiae* genome using the primers OIT2393 (5′-TAGATGGGATCCATGTCCTTCTTTGGGTTAGAAAATAGCGG-3′) and OIT2394 (5′-TTGAACGTCGACTTACGCGTAGTCTGGGACGTCGTATGGGTACTTTAGTTCTGATATTTCACCATCGCGA-3′) and inserted between BamHI and SalI sites in p*GPD1p*. To construct pIT2145 (p*GPDp-NOT1-HA*), the *NOT1* gene was amplified from *S. cerevisiae* genome using the primers OIT2448 (5′- TAGATGGAATTCATGCTATCGGCCACATACCGTGATTTGAAC-3′) and OIT2392 (5′- TTGAACGTCGACTTACGCGTAGTCTGGGACGTCGTATGGGTATGCGTTGGATTGTAGAGGGGTTTGCCT-3′) and inserted between EcoRI and SalI sites in p*GPD1p*.

Tethering Assay in Zebrafish Embryos—Tethering assay in zebrafish embryos was performed as described previously (40) with some modifications. mRNAs were transcribed using an mMessage mMachine SP6 kit (Ambion). A-capped mRNA was synthesized in the presence of an ApppG cap analogue (New England Biolabs) instead of an m7GpppG cap analogue. To block polyadenylation and translation of the GFP reporter mRNA in zebrafish embryos, we injected MOs that bind to the 3′-end of the GFP reporter mRNA (PB MO; GGTACCGGGCCCAATGCATTGGCGC) and translation block MO that binds to the start codon (ACAGCTCCTCGCCCTTGCTCACCAT). MOs were purchased from Gene Tools. For mRNA injections, GFP mRNA and Fluc mRNA were diluted to a final concentration of 50 ng/μl each. HA-λN-Mid mRNA was diluted to a final concentration of 100 ng/μl. Approximately 1,000 pl of solution containing reporter mRNAs and effector mRNAs was injected into one-cell stage zebrafish embryos. A total of 10 embryos were collected at 10 h after injection, and total RNA was extracted with Isogen (NipponGene).

Poly(A) Tail Analysis—To analyze poly(A) tail length of the endogenous mRNAs, we followed the protocol of Hire-PAT (52) with the following modifications. Purified total RNA was treated with yeast PAP (Affymetrix) in the presence of 0.375 mM GTP and 0.125 mM ITP at 37 °C for 1 h. cDNA was synthesized with Perfect RT gEraser (TAKARA) according to the manufacturer's protocol except for the primer used (PAT reverse primer) and incubation temperature (44 °C). PCR was performed using GoTaq (Promega) and the primers listed below for 30–32 cycles. PCR products were separated on 6% polyacrylamide gel with 0.5× TBE, stained with GelRed (WAKO), and visualized with a LAS3000 imager (GE Healthcare). PCR products were cloned into pCRII TOPO (Invitrogen), and sequences were confirmed.

Overexpression of Dominant Negative CNOT7 and DCP2 and Inhibition of miR-430—ORFs of zebrafish *cnot7* (ENSDART00000092953) and *dcp2* (ENSDART00000056951) were amplified by RT-PCR and cloned into pCS2+MT vector. The following mutations were introduced to make a dominant-negative form of each protein: CNOT7, D40A/E42A (catalytic core) and C67E/L71E (CNOT6 interaction surface); DCP2, E147A/E148A (catalytic core). mRNAs were transcribed using a mMessage mMachine SP6 kit (Ambion) and diluted to a final concentration of 250 ng/μl. Approximately 1,000 pl of solution was injected into one-cell stage zebrafish embryos. To inhibit zebrafish miR-430, a mixture of morpholinos that targets miR-430a (final concentration 0.286 mM), miR-430b (143 mM), and miR-430c (71 mM) was injected at the one-cell stage. miR-430 MO sequences are as follows: miR-430a MO, ACTACCCCAACAAATAGCACTTACC; miR-430b MO, TCTACCCCAACTTGATAGCACTTTC; miR-430c MO, ACTACCCCAAAGAGAAGCACTTATG.

qRT-PCR—qRT-PCR was performed as described previously (40) using the primers in Table 2. Specific amplification was confirmed by analyzing the dissociation curve and sequencing. For the analysis of endogenous miR-430 targets, values in each injection experiment were normalized by the value of *actb1*. The normalized value in the miR-430 MO injection experiment was set to 1. Experiments were repeated three times.

Circularized Rapid Amplification of cDNA Ends (cRACE)—cRACE was performed essentially as described previously (53) with some modifications. Briefly, 4–5 μg of zebrafish total RNA was treated with 10 units of calf intestine alkaline phosphatase (TAKARA) for 1 h at 37 °C and extracted with phenol-chloroform. RNA was then decapped with 10 units of tobacco acid pyrophosphatase (Epicenter Biotechnologies) for 1 h at 37 °C and extracted with phenol-chloroform. We then incubated decapped RNA or an equivalent amount of naive RNA with 20 units of T4 RNA ligase (New England Biolabs) in a 120-μl reaction at 20 °C for 16 h. RNA samples were extracted with phenol-

chloroform, and one-forth of the ligation products were used to make cDNA with Superscript III (Invitrogen) using eif4ebp-specific primer: 5′-CAGGGCTCACAGGTTAACTTTC-3′. First and second PCR were performed with the following primers for 22 cycles each: first primer, 5′-GCTGAGCAGCTGTGTCAAATAC-3′ (forward) and 5′-CAGGGCTCACAGGTTAACTTTC-3′ (reverse); second primer, 5′-CCGCTCGAGTTCAAGTGGAGAACAAGATCAAG-3′ (forward) and 5′-CCGGAATTCGGTATCTACAAGCCAAGCCACT-3′ (reverse). PCR products with expected size (0.8–1.2 kb) were excised and cloned into pBluescript II (SK^+) with EcoRI and XhoI. Clones were analyzed by sequencing from both ends of amplicons. Clones containing the expected 3′ ends followed by a poly(A) tail and the expected 5′ sequence in this order were considered as intramolecularly ligated products and included in the analysis.

RESULTS

Tethered TNRC6A Recapitulates Hallmarks of miRNA-mediated Gene Silencing in S. cerevisiae—To elucidate the roles of the CCR4-NOT complex, which is recruited by GW182/TNRC6 in both mRNA decay and translation repression, we attempted to recapitulate the gene silencing activities of GW182/TNRC6 in yeast. First, we examined the interaction of the carboxyl-terminal region of zebrafish TNRC6A (Mid domain; amino acids 1310–1567) (40), which was sufficient for translation repression and deadenylation in zebrafish embryos, with the yeast CCR4-NOT complex (Fig. 1, *A* and *B*). HA-tagged Not1 and Ccr4 proteins, subunits of the yeast CCR4-NOT complex, co-immunoprecipitated with FLAG-tagged MS2 protein fused to the Mid domain (F-MS2-Mid) (Fig. 1, *B* and *C*, *lanes 4* and *5*). Introduction of alanine mutations in the CIM1 and W-motifs that disrupted the interaction between CNOT1 and GW182/TNRC6 in human and *Drosophila* cells (33, 34) (F-MS2-Mid-M) weakened the interaction of the zebrafish Mid domain with Not1 and Ccr4 (Fig. 1, *B* and *C*, *lanes 5* and *6*), although the expression levels of these proteins were comparable (Fig. 1*D*). We next examined the effects of F-MS2-Mid on the levels of mRNA and protein expressed from *GFP* reporter genes containing MS2 binding sites. To determine whether a poly(A) tail was required, we inserted the sequence of a hammerhead ribozyme (*Rz*) downstream of the MS2 binding sites (Fig. 1*E*) (49). Tethering of F-MS2-Mid reduced the levels of *GFP-MS2* and *GFP-MS2-Rz* reporter mRNAs (Fig. 1*F*, *lanes 3* and *4* and *lanes 7* and *8*), whereas tethering of F-MS2-Mid-M did not (Fig. 1*F*, *lanes 7* and *8* and *lanes 11* and *12*). Likewise, tethering of F-MS2-Mid reduced the protein levels derived from *GFP-MS2* or *GFP-MS2-Rz* reporters, whereas tethering of F-MS2-Mid-M did not (Fig. 1*G*, *lanes 7* and *8* and *lanes 11* and *12*). Polysome analysis using sucrose density gradients revealed that levels of *GFP-MS2* and *GFP-MS2-Rz* mRNAs reduced in the polysome fraction but increased in the 80S monosome and free fractions in cells expressing the F-MS2-Mid protein relative to cells expressing the control MS2 protein (Fig. 1*H*, Student's *t* test, $p < 0.05$). To directly examine translation repression by the tethered Mid domain of zebrafish TNRC6, we performed pulse-labeling experiments. Levels of synthesized GFP derived from reporter mRNAs were significantly decreased by tethered TNRC6A (Fig. 1*I*). The corresponding region of *Drosophila* GW182 also induced gene silencing in yeast (data not shown). These results indicate that tethered TNRC6 protein fragments reduced both translation efficiency and mRNA levels by recruiting the CCR4-NOT complex in *S. cerevisiae* in a poly(A) tail-independent manner.

Tethered TNRC6 Stimulates the Degradation of mRNA from the 5′ End, Independent of Translation and a Poly(A) Tail—We next examined the effects of F-MS2-Mid on mRNA stability, using reporter genes containing an ORF of N-terminally truncated *MPT4* (473 nucleotides) and MS2 binding sites, as described previously (Fig. 2*A*) (49). Consistent with the results obtained using GFP reporter mRNAs (Fig. 1*F*), half-life analysis revealed that tethered Mid domain dramatically stimulated mRNA degradation in a poly(A) tail-independent manner (Fig. 2*B*, wild type). Degradation was dependent on the 5′–3′ exonuclease Xrn1 but not the 3′–5′ exosome component Ski2, indicating that degradation occurred from the 5′ end (Fig. 2*B*). To dissect the effects of the tethered Mid domain on translation, deadenylation, and mRNA decay, we utilized previously constructed reporters containing MS2 binding sites. These constructs were of two types: the *No-AUG-MS2* reporters are not translated because all AUG codons in the ORF of N-terminally truncated *MPT4* were replaced with UAC codons (Fig. 2*A*), and the *-Rz* reporters lack a poly(A) tail (Fig. 2*A*) (49). The tethering of F-MS2-Mid reduced the levels of both *No-AUG-MS2* and *No-AUG-MS2-Rz* reporter mRNAs, and this down-regulation was mediated by the CCR4-NOT complex (Fig. 2*C*). Half-life analysis revealed that tethering of the Mid domain accelerated the decay rate of *No-AUG-MS2-Rz* mRNA via an interaction with the CCR4-NOT complex (Fig. 2*D*, $t_{1/2} = 3.9$ min, F-MS2-Mid *versus* $t_{1/2} = 8.1$ min, F-MS2-Mid-M). Destabilization of *No-AUG-MS2-Rz* mRNA by F-MS2-Mid was significantly suppressed in *xrn1*Δ mutant cells (Fig. 2*D*, $t_{1/2} > 16$ min) but not in *ski2*Δ mutant cells (Fig. 2*D*, $t_{1/2} = 4.1$ min), further confirming that the Mid domain stimulates 5′-to-3′ mRNA decay. The *Rz-No-AUG-MS2-Rz* mRNA, which lacks a cap structure and is therefore intrinsically unstable, was not further destabilized by the tethering of F-MS2-Mid (Fig. 2*E*). Overall, these experiments suggest that in yeast, tethering of the Mid domain of zebrafish TNRC6A stimulates 5′-to-3′ degradation of the reporter mRNA independent of translation and a poly(A) tail.

To investigate whether the decapping reaction would be accelerated by the Mid domain of zebrafish TNRC6A, we measured the levels of the decapped reporter mRNA (Fig. 3*A*). To this end, we utilized *xrn1*Δ mutant cells in which decapped mRNAs are stabilized and consequently accumulate. By treating purified RNA with Terminator exonuclease, which specifically degrades 5′-monophosphorylated RNA, the levels of decapped mRNAs could be estimated (54). In the control tethering experiment with F-MS2, the level of *No-AUG-MS2-Rz* mRNA was reduced to 59% by Terminator treatment, revealing that the decapped fraction was 41% (Fig. 3*B*, *lanes 1* and *2*; see also Fig. 3*C* for quantitation, Student's *t* test, $p < 0.05$). By contrast, Terminator exonuclease reduced the reporter mRNA tethered by F-MS2-Mid to 21%, indicating that ~80% of the reporter mRNA was decapped by the Mid domain (Fig. 3*B*,

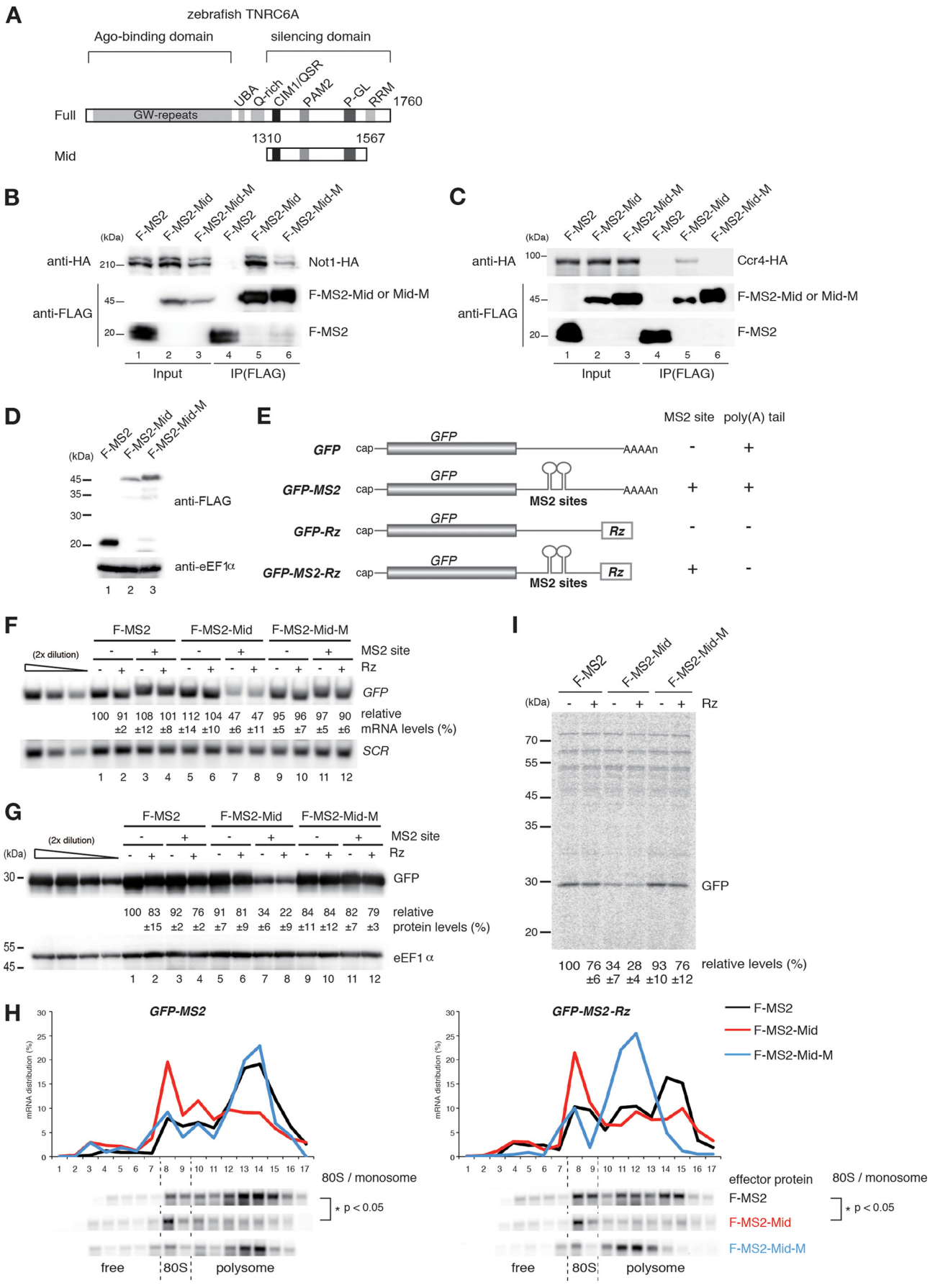
A
zebrafish TNRC6A
Ago-binding domain
silencing domain
UBA
Q-rich
CIM1/QSR
PAM2
P-GL
RRM
1760
Full
GW-repeats
1310
1567
Mid
B
(kDa)
F-MS2
F-MS2-Mid
F-MS2-Mid-M
F-MS2
F-MS2-Mid
F-MS2-Mid-M
anti-HA
210
Not1-HA
anti-FLAG
45
F-MS2-Mid or Mid-M
20
F-MS2
1 2 3 4 5 6
Input
IP(FLAG)
C
(kDa)
F-MS2
F-MS2-Mid
F-MS2-Mid-M
F-MS2
F-MS2-Mid
F-MS2-Mid-M
anti-HA
100
Ccr4-HA
anti-FLAG
45
F-MS2-Mid or Mid-M
20
F-MS2
1 2 3 4 5 6
Input
IP(FLAG)
D
(kDa)
F-MS2
F-MS2-Mid
F-MS2-Mid-M
45
35
30
20
anti-FLAG
anti-eEF1α
1 2 3
E
MS2 site
poly(A) tail
GFP
cap
GFP
AAAAn
-
+
GFP-MS2
cap
GFP
MS2 sites
AAAAn
+
+
GFP-Rz
cap
GFP
Rz
-
-
GFP-MS2-Rz
cap
GFP
MS2 sites
Rz
+
-
F
F-MS2
F-MS2-Mid
F-MS2-Mid-M
(2x dilution)
MS2 site
Rz
GFP
100 91 108 101 112 104 47 47 95 96 97 90
±2 ±12 ±8 ±14 ±10 ±6 ±11 ±5 ±7 ±5 ±6
relative mRNA levels (%)
SCR
1 2 3 4 5 6 7 8 9 10 11 12
G
F-MS2
F-MS2-Mid
F-MS2-Mid-M
(2x dilution)
(kDa)
MS2 site
Rz
30
GFP
100 83 92 76 91 81 34 22 84 84 82 79
±15 ±2 ±2 ±7 ±9 ±6 ±9 ±11 ±12 ±7 ±3
relative protein levels (%)
55
45
eEF1 α
1 2 3 4 5 6 7 8 9 10 11 12
I
F-MS2
F-MS2-Mid
F-MS2-Mid-M
(kDa)
Rz
70
55
45
35
30
GFP
20
100 76 34 28 93 76
±6 ±7 ±4 ±10 ±12
relative levels (%)
H
GFP-MS2
mRNA distribution (%)
80S / monosome
* p < 0.05
free
80S
polysome
GFP-MS2-Rz
F-MS2
F-MS2-Mid
F-MS2-Mid-M
effector protein
F-MS2
F-MS2-Mid
F-MS2-Mid-M
80S / monosome
* p < 0.05
free
80S
polysome

lanes 5 and *6*; see also Fig. 3*C* for quantitation, Student's *t* test, $p < 0.01$). The levels of endogenous *RPL28* mRNA were reduced equally by Terminator exonuclease regardless of the tethering construct (Fig. 3*B*, *lanes 1* and *2* and *lanes 5* and *6*; see also Fig. 3*D*). After the removal of the cap structure by treatment with tobacco acid pyrophosphatase, *RPL28* and *No-AUG-MS2-Rz* mRNA were almost completely degraded by Terminator exonuclease (Fig. 3, *B–E*). A spiked 5′-triphosphorylated *GFP* RNA produced by *in vitro* transcription was not degraded by Terminator nuclease, confirming the enzyme's substrate specificity (Fig. 3, *B* and *D*). No difference was observed between F-MS2 and F-MS2-Mid in wild type cells, in which decapped mRNAs do not accumulate (Fig. 3, *D* and *E*). These results indicate that tethering of F-MS2-Mid stimulates the decapping reaction, followed by rapid degradation of the reporter mRNA from 5′ end by Xrn1, independent of translation and a poly(A) tail.

Zebrafish miR-430 Stimulates mRNA Decay When the Deadenylase Activity of the CCR4-NOT Complex Is Inhibited—The results described above imply that TNRC6 can stimulate mRNA decay in a decapping-dependent but a poly(A) tail- and translation-independent manner. A similar observation regarding activation of decapping by miRISC has been reported in *Drosophila* S2 cells (25, 26, 28), supporting our findings in the hybrid assay system. Therefore, we performed three experiments in zebrafish embryos to assess the validity of our findings in yeast. First, we asked whether TNRC6A would destabilize bound mRNAs in zebrafish embryos independently of translation and a poly(A) tail. To address this question, we injected *GFP* reporter mRNA into zebrafish embryos and then blocked its translation using a morpholino oligomer (*ATG MO*) that specifically masks the start codon of the *GFP* ORF (Fig. 4*A*). In addition, we used a poly(A) tail-blocking MO (*PB MO*) that binds to the 3′ end of *GFP* mRNA to inhibit cytoplasmic polyadenylation during zebrafish embryogenesis (Fig. 4, *B* and *C*) (55). We then asked whether tethering of the Mid domain fused with the λN peptide to a *GFP* mRNA containing the BoxB sequence promotes mRNA decay independent of translation and a poly(A) tail. qRT-PCR analysis of reporter mRNA 10 h after injection revealed that, relative to the control tethering experiment using λN-MS2, tethering of the Mid domain promoted mRNA decay of an m^7G-capped reporter mRNA whose translation and a poly(A) tail were blocked (Student's *t* test, $p < 0.01$; Fig. 4, *D* (*left*) and *E*). To determine whether this was due to the stimulation of decapping, we replaced the m^7G cap with an A cap, because the decapping enzyme Dcp2 removes non-methylated cap structures less efficiently *in vitro* (56). The stability of the A-capped reporter mRNA was not significantly changed by the Mid domain (Student's *t* test, $p = 0.53$; Fig. 4, *D* (*right*) and *E*). These results show that the Mid domain of TNRC6A promotes mRNA decay by decapping in a translation- and poly(A) tail-independent manner in zebrafish embryos.

Second, we asked whether stimulation of target mRNA decapping contributes to the miRNA-mediated mRNA decay *in vivo*. We reasoned that if miRISC directly activates decapping, deadenylation should not be prerequisite for mRNA decay. To test this idea, we blocked miRNA-mediated deadenylation by overexpressing a mutant CNOT7 protein that lacks deadenylase activity (5) and cannot recruit the other deadenylase subunit CCR4/CNOT6 to CNOT1 (4, 5, 42). To monitor miRNA-mediated mRNA degradation, we measured the levels of three miR-430 target mRNAs (*eif4ebp2*, *gstm*, and *acadl*) at 6 h postfertilization, when miR-430 target mRNAs are degraded (22, 52). Overexpression of the CNOT7 mutant indeed inhibited deadenylation by miR-430, albeit not as efficiently as miR-430 antisense MO (Fig. 4*F*). qRT-PCR analysis revealed that inhibition of deadenylation caused accumulation of the three mRNAs to different extents (Fig. 4, *G* and *H*); in particular, although statistically significant (Student's *t* test, $p < 0.05$), *eif4ebp2* appeared less sensitive to the deadenylation inhibition. Inhibition of decapping by overexpression of catalytically inactive DCP2 (56) stabilized *eif4ebp2* and *acadl* mRNAs (Student's *t* test, $p < 0.05$) but again to different extents (Fig. 4, *F* and *G*). These results suggest that mRNAs such as *eif4ebp2* are degraded by miR-430 in a manner that is less dependent on deadenylation but still dependent on decapping.

Third, we simultaneously captured both 5′ and 3′ ends of *eif4ebp2* mRNA in wild type and CNOT7 DN expressed embryos at 5 h postfertilization by cRACE (53) to directly ask whether miR-430 produced decapped but polyadenylated decay intermediates. When cRACE was performed with RNA samples pretreated with calf intestine alkaline phosphatase followed by tobacco acid pyrophosphatase, capped 5′ ends that were intramolecularly ligated to 3′-OH ends could be captured (53). Indeed, amplicons from calf intestine alkaline phosphatase/tobacco acid pyrophosphatase-treated RNA samples contained 3′-to-5′ ligation junctions that converged at two 5′ sites

FIGURE 1. **Tethered TNRC6A recapitulates hallmarks of miRNA-mediated gene silencing in *S. cerevisiae*.** *A*, schematic structures of zebrafish TNRC6A and its Mid domain. *B* and *C*, interaction of FLAG-MS2-TNRC6A Mid with yeast Not1-HA and Ccr4-HA. Cell lysates of wild type cells transformed with the indicated plasmids were immunoprecipitated using anti-FLAG antibody. Total extracts (*Input*) and immunoprecipitates (*IP*) were analyzed by Western blotting using anti-HA or anti-FLAG antibody. *D*, the expression of the Mid domain of zebrafish TNRC6A in yeast. FLAG-tagged effector proteins were analyzed by Western blotting using anti-FLAG antibody. *F-MS2*, FLAG-MS2 protein; *F-MS2-Mid*, FLAG-MS2-TNRC6Amid fusion protein; *F-MS2-Mid-M*, FLAG-MS2-TNRC6Amid QSR and W mutant fusion protein. This mutant contains the mutations that disrupt the interaction of Not1 with TNRC6. *E*, schematic drawing of reporter genes used in Fig. 1. The *filled box* indicates the open reading frame. All reporter genes contain the 3′-UTR region of PGK1, in which two tandem MS2 binding sites were inserted. *Rz*, a hammerhead ribozyme that generates a 3′ end with no poly(A) tail. *F*, tethering of TNRC6A reduces mRNA levels independently of a poly(A) tail. RNA samples from wild type cells transformed with the indicated plasmids were analyzed by Northern blotting using *GFP* and *SCR* probes. The data represent the means of three independent experiments, with S.D. values. *G*, tethering of TNRC6Amid reduces protein levels independently of a poly(A) tail. Wild type cells harboring the indicated plasmids were grown, and protein samples were analyzed by Western blotting using anti-GFP antibody. eEF1α served as a loading control. The data represent the means of three independent experiments with S.D. values. *H*, tethering of TNRC6A induces translation repression, dependent on interaction with Not1 but independent of a poly(A) tail. Cell extracts were prepared from wild type cells transformed with the indicated plasmids, and polysome analysis was performed. *Top*, ratio (%) of mRNA distribution in each fraction. *Bottom*, reporter mRNA was detected by Northern blotting using a *PGK1* 3′UTR probe. The *p* value was calculated by using Student's *t* test. *I*, levels of synthesized GFP derived from reporter mRNAs were significantly reduced by tethered TNRC6 independently of a poly(A) tail. Pulse-labeling experiments were performed using the same cells as in F. GFP-MS2 and GFP-MS2-Rz protein levels are shown as the mean values of three independent experiments with S.D. values.

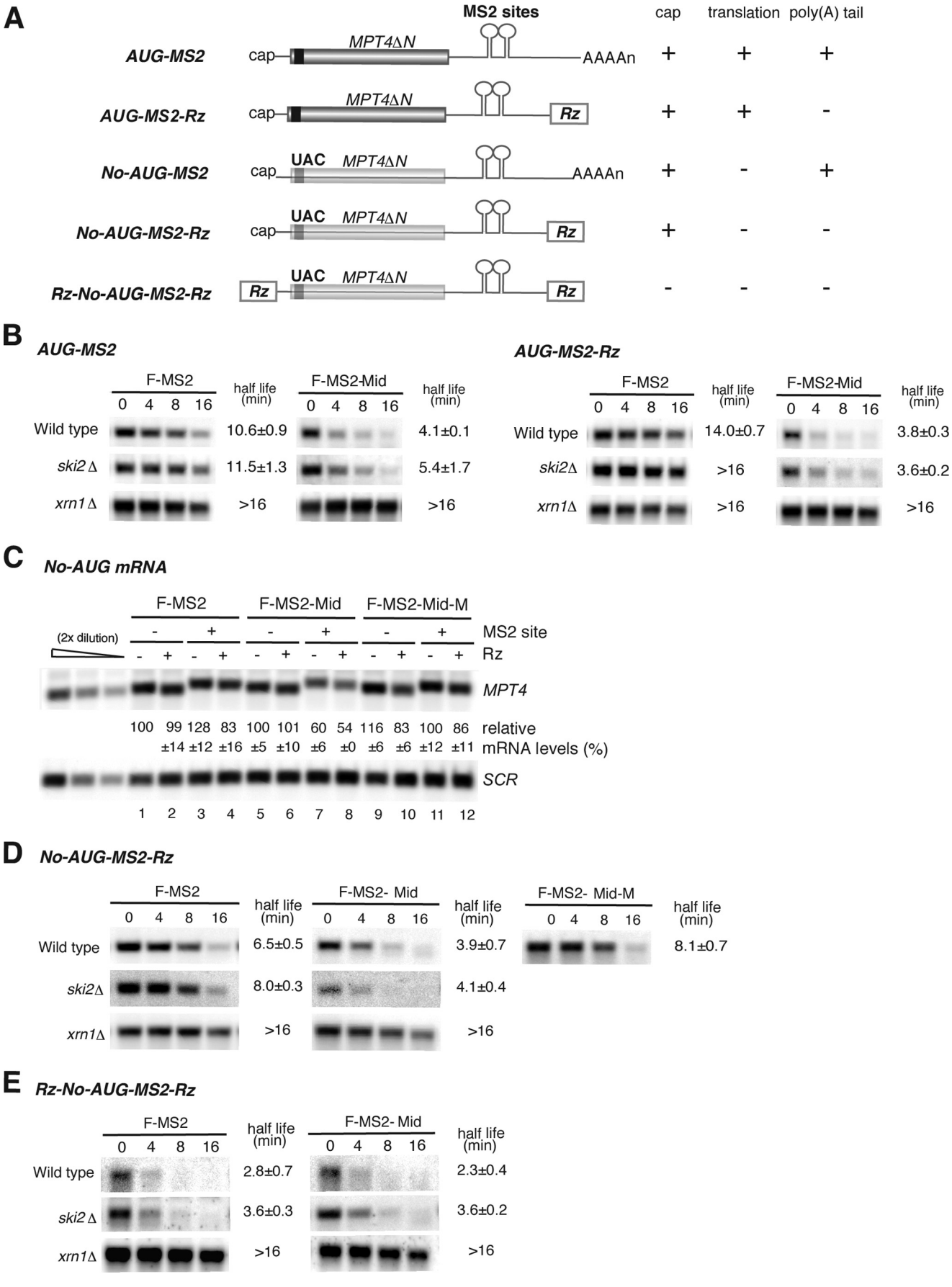
A
MS2 sites
cap
translation
poly(A) tail
AUG-MS2
MPT4ΔN
cap
AAAAn
+ + +
AUG-MS2-Rz
Rz
+ + -
No-AUG-MS2
UAC
+ - +
No-AUG-MS2-Rz
+ - -
Rz-No-AUG-MS2-Rz
- - -
B
AUG-MS2
F-MS2
F-MS2-Mid
0 4 8 16
half life (min)
Wild type
10.6±0.9
4.1±0.1
ski2Δ
11.5±1.3
5.4±1.7
xrn1Δ
>16
>16
AUG-MS2-Rz
Wild type
14.0±0.7
3.8±0.3
ski2Δ
>16
3.6±0.2
xrn1Δ
>16
>16
C
No-AUG mRNA
F-MS2
F-MS2-Mid
F-MS2-Mid-M
(2x dilution)
MS2 site
Rz
MPT4
100 99 128 83 100 101 60 54 116 83 100 86
±14 ±12 ±16 ±5 ±10 ±6 ±0 ±6 ±6 ±12 ±11
relative mRNA levels (%)
SCR
1 2 3 4 5 6 7 8 9 10 11 12
D
No-AUG-MS2-Rz
F-MS2
F-MS2- Mid
F-MS2- Mid-M
0 4 8 16
half life (min)
Wild type
6.5±0.5
3.9±0.7
8.1±0.7
ski2Δ
8.0±0.3
4.1±0.4
xrn1Δ
>16
>16
E
Rz-No-AUG-MS2-Rz
F-MS2
F-MS2- Mid
0 4 8 16
half life (min)
Wild type
2.8±0.7
2.3±0.4
ski2Δ
3.6±0.3
3.6±0.2
xrn1Δ
>16
>16

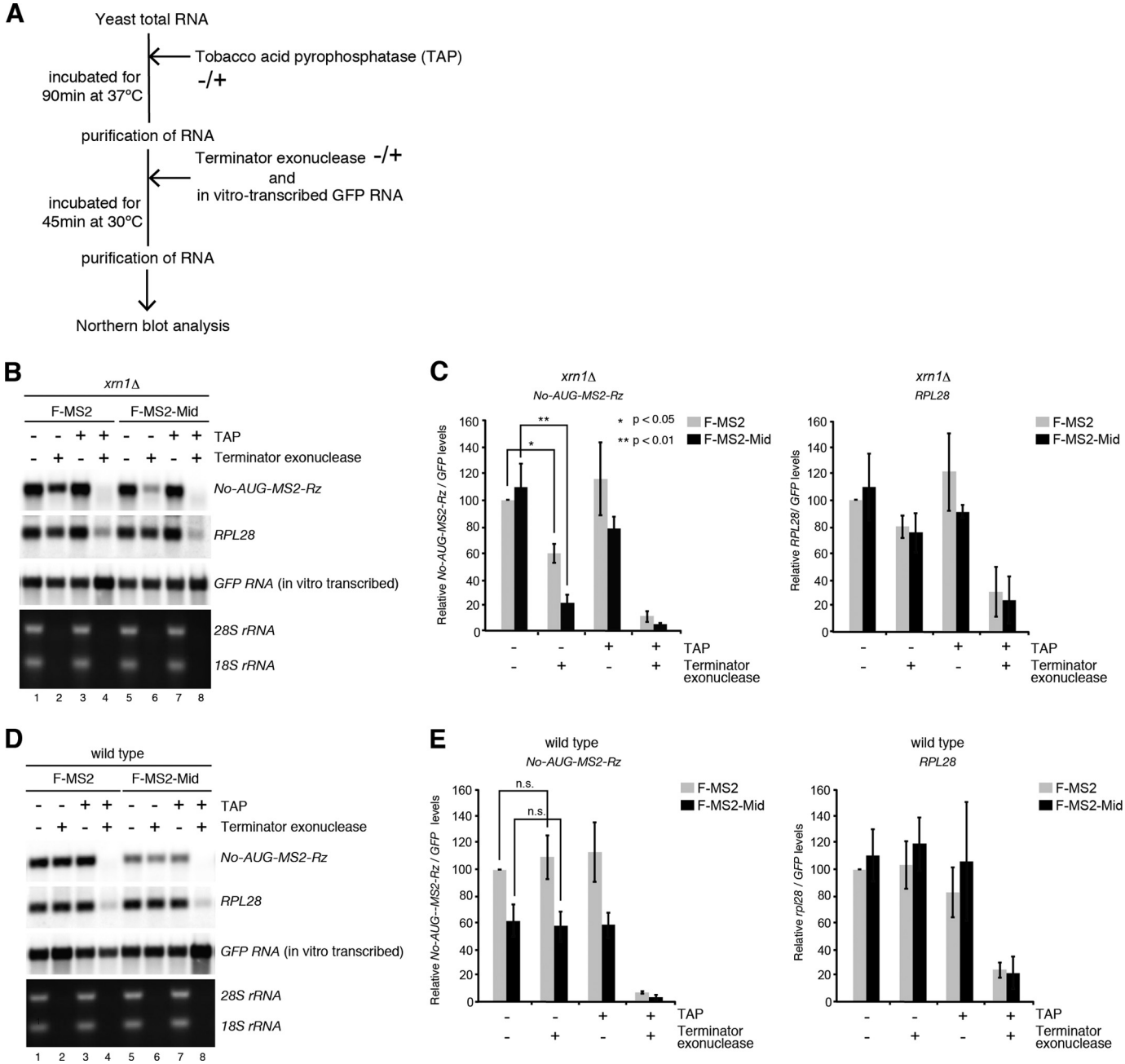

FIGURE 3. **Tethered TNRC6A stimulates the decapping reaction independent of translation and a poly(A) tail.** *A*, schematic of the experimental procedure. *B* and *D*, TNRC6A promotes the decapping reaction, independent of translation and a poly(A) tail. RNA samples were prepared from wild type and *xrn1*Δ cells harboring the *No-AUG-MS2-Rz* reporter gene and then incubated in the absence or presence of Terminator exonuclease and tobacco acid pyrophosphatase (*TAP*). *In vitro* transcribed 5′-triphosphate *GFP* RNA was added after tobacco acid pyrophosphatase treatment. RNA samples were analyzed by Northern blotting. *C* and *E*, quantitation of the levels of *No-AUG-MS2-Rz* reporter (*left*) and *rpl28* mRNAs (*right*). The levels of reporter and *rpl28* mRNAs were normalized to those of the control *GFP* RNA as described in *B* and *D*. *Error bars*, S.D. The *p* value was calculated by using Student's *t* test.

FIGURE 2. **Tethered TNRC6A stimulates decapping and the degradation of mRNA from the 5′ end, independent of translation and a poly(A) tail.** *A*, schematic drawing of reporter genes used in Fig. 2. The *line* represents non-translated regions. All reporter genes contain the 3′-UTR region of *PGK1*, in which two tandem MS2 binding sites were inserted. *B*, tethering of TNRC6A stimulates 5′-to-3′ mRNA decay independent of a poly(A) tail. Wild type, *ski2*Δ, and *xrn1*Δ cells containing the indicated reporter gene and plasmids were grown, RNA samples were purified at each time point, and the reporter mRNA was analyzed by Northern blotting using a DIG-labeled *PGK1* 3′-UTR probe. *C*, TNRC6A reduces mRNA levels independently of translation and a poly(A) tail. Wild type cells harboring the indicated *No-AUG* reporter genes were grown, and RNA samples were analyzed by Northern blotting using a DIG-labeled *MPT4* probe. The data represent the means of three independent experiments with S.D. values**.** *D* and *E*, tethering of the Mid domain of TNRC6A promotes 5′-to-3′ mRNA decay independent of translation and a poly(A) tail in a cap-dependent manner. Wild type, *ski2*Δ, and *xrn1*Δ cells harboring *No-AUG-MS2-Rz* (*D*) and *Rz-No-AUG-MS2-Rz* (*E*) reporter gene and plasmids were grown, and RNA samples were analyzed by Northern blotting using a DIG-labeled *PGK1* 3′-UTR probe. The half-lives of mRNA in the indicated cells are shown as the mean values of three independent experiments with S.D. values.

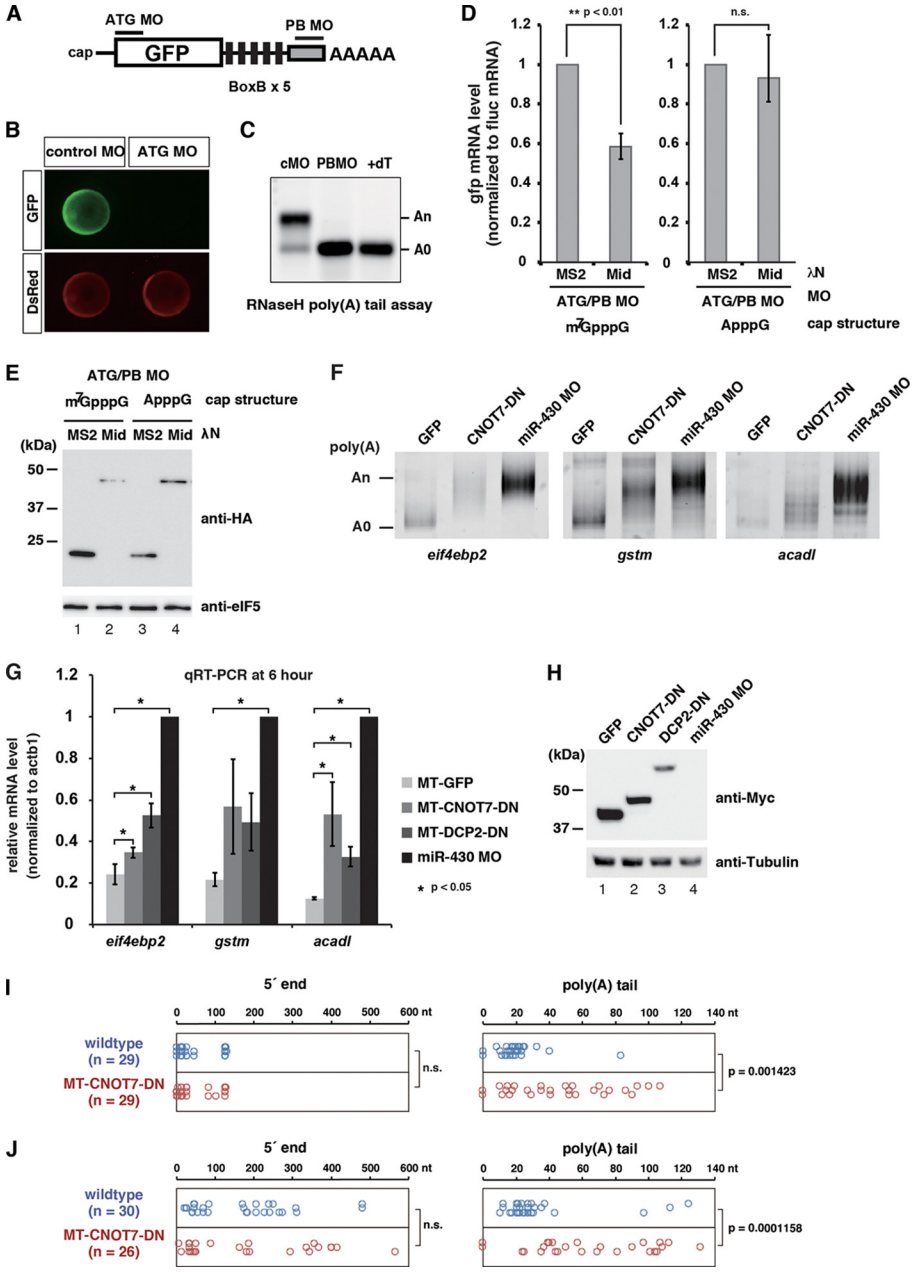

FIGURE 4. **Validation of the deadenylation-independent mRNA decay pathway in zebrafish embryos.** *A*, schematic representations of the *GFP* reporter mRNA with BoxB sites and MOs used to analyze translation- and a poly(A) tail-independent mRNA decay by the TNRC6A Mid domain in zebrafish embryos. The translation-blocking MO (*ATG MO*) specifically masks the start codon of the GFP ORF. The polyadenylation-blocking MO (*PB MO*) binds to the end of the *GFP* mRNA and inhibits cytoplasmic polyadenylation during zebrafish embryogenesis. *B*, confirmation of the effect of ATG MO in zebrafish embryos. *GFP* and *DsRed* mRNAs were co-injected with MOs at the one-cell stage. GFP expression from the *GFP* reporter mRNA was completely blocked by ATG MO (*green*). Translation of co-injected *DsRed* mRNA was unaffected (*red*). Embryos are shown 10 h postfertilization. *C*, confirmation of the effect of PB MO in zebrafish embryos. *GFP* mRNA without a poly(A) tail was co-injected with MOs at the one-cell stage. The poly(A) tail length of the *GFP* mRNA was analyzed 4 h postfertilization by RNase H digestion and Northern blotting. Injected mRNA was polyadenylated after injection in the presence of control MO. PB MO completely blocked polyadenylation of the *GFP* mRNA. +*dT*, RNase H-treated sample in the presence of oligo(dT) (15), representing the completely deadenylated A(0) fragment. *D*, stability of the injected *GFP* reporter mRNA was determined by qRT-PCR 10 h after injection. *Left*, qRT-PCR analysis of the stability of reporter mRNA containing the 5′ m^7G-cap. *Right*, qRT-PCR analysis of the stability of reporter mRNA containing the 5′ A-cap. *GFP* mRNA values were normalized against *Fluc* mRNA values. Normalized values of the experiments using HA-λN MS2 were set to 1. Graphs represent the means of three independent experiments. *Error bars*, S.D. The *p* value was calculated by using Student's *t* test. *E*, HA- and λN-tagged effector proteins used in *D* were detected by Western blotting using anti-HA antibody. eIF5 was served as loading control. *F*, poly(A) tail analysis of the endogenous miR-430 target mRNAs at 6 h postfertilization. mRNA encoding GFP or dominant-negative CNOT7 or MO against miR-430 was injected at the one-cell stage as indicated. The putative position of the A(0) product is shown on the *left*. *G*, qRT-PCR analysis of the miR-430 target mRNAs at 6 h postfertilization in the presence of GFP, dominant negative CNOT7, dominant negative DCP2, or miR-430 MO. mRNA levels were normalized against *actb1*. Normalized values of the experiments using miR-430 MO were set to 1. Graphs represent the means of three independent experiments. *Error bars*, S.D. The *p* value was calculated by using Student's *t* test. *H*, Myc-tagged effector proteins used in *F* and *G* were detected by Western blotting using anti-Myc antibody. Tubulin was served as loading control. *I* and *J*, cRACE analysis of *eif4ebp2* mRNA at 5 h postfertilization in wild type (*blue*) and dominant negative CNOT7-injected embryos (*red*). *Left panels*, nucleotide position of 5′ end ligation junctions relative to the annotated *eif4ebp2* transcript (ENSDART00000040926). *Right panels*, poly(A) tail length between the annotated 3′-UTR and ligated 5′ end. *I*, results of cRACE capturing capped mRNA; *J*, results of cRACE capturing decapped mRNA. The *p* value was calculated by using the Wilcoxon-Mann-Whitney test. n.s., not significant.

of *eif4ebp2* mRNA, presumably representing two alternative transcriptional start sites (Fig. 4*I*, *left*). Analysis of these amplicons revealed that 3′ ends of capped *eif4ebp2* mRNA were mostly deadenylated (<30-nucleotide poly(A) tail) in wild type (Fig. 4*I*, *right*). On the other hand, longer poly(A) tail was retained in CNOT7 DN expressed embryos (Wilcoxon-Mann-Whitney test, $p < 0.01$), consistent with the poly(A) tail analysis in Fig. 4*F*. We then performed cRACE with naive RNA samples to capture 5′-monophosphate ends that were ligated to 3′-OH ends. Under this experimental condition, ligation junctions from both wild type and CNOT7 DN expressed embryos were located downstream of major transcriptional start sites and were broadly distributed (Fig. 4*J*, *left*), representing decapped RNA molecules being degraded in the 5′-to-3′ direction (53). Notably, the poly(A) tail length of decapped *eif4ebp2* mRNA was significantly longer in CNOT7 DN expressed embryos compared with wild type (Fig. 4*J*, *right*, $p < 0.01$), as observed with capped *eif4ebp2* mRNA. Indeed, >50% of decapped *eif4ebp2* mRNA still retained a >50-nucleotide poly(A) tail in CNOT7 DN expressed embryos. This result further supported the idea that *eif4ebp2* mRNA was degraded from the 5′ end by miR-430-mediated decapping even if efficient deadenylation was not ensured. Overall, these experiments confirmed that miR-430 is capable of inducing decapping and 5′-to-3′ decay independent of deadenylation in zebrafish embryos.

mRNA Decapping Factors Exert Partially Redundant Functions in Rapid mRNA Decay from the 5′ End by Tethered TNRC6—Based on the results described above and those of previous studies (25, 28, 38, 57, 58), we hypothesized that the tethered Mid domain recruits yeast CCR4-NOT complex by interacting with mRNA fate modulators, such as Dhh1 and Pat1, thereby stimulating the decapping reaction. To address this possibility, we first confirmed the interaction between FLAG-tagged F-MS2-Mid and HA-tagged Dhh1 and Pat1. Dhh1-HA protein co-immunoprecipitated with F-MS2-Mid, whereas HA-tagged Pat1 did not (Fig. 5*A*, *lanes 3* and *4*). Consistent with previous reports, HA-tagged Not1 co-immunoprecipitated with FLAG-tagged Dhh1 (Fig. 5*B*) (8). We then measured the stability of *No-AUG-MS2-Rz* mRNA in decapping activator mutants. *No-AUG-MS2-Rz* mRNA was dramatically stabilized in the *dhh1*Δ*pat1*Δ double mutant (Fig. 5*C*, Student's *t* test, *n.s.*) but not in the *dhh1*Δ or *pat1*Δ single mutants (Fig. 5*C*, Student's *t* test, $p < 0.01$). These results provided genetic evidence that Dhh1 and Pat1 play overlapping roles in destabilization of the reporter mRNA by the CCR4-NOT complex recruited by TNRC6A.

Distinct Roles of mRNA Decapping Factors in Translation Repression and Rapid mRNA Decay from the 5′ End by Tethered TNRC6—The CCR4-NOT complex has been suggested to play a role in miRNA-mediated translation repression (34, 35), and the mRNA fate modulators Dhh1 and Pat1 are also translational repressors (15–17). Furthermore, involvement of DDX6 in miRNA-mediated translation repression has been reported (11, 12, 43, 59). Therefore, we examined the roles of CCR4-NOT and decapping components in translation repression by the Mid domain. First, we performed polysome analysis to confirm that CCR4-NOT components are required for translation repression by tethered TNRC6A in yeast. Translation repression of *AUG-MS2* and *AUG-MS2-Rz* mRNA by tethered F-MS2-Mid was almost abolished in *ccr4*Δ and *caf1*Δ mutant cells in comparison with wild type cells, independent of a poly(A) tail (Fig. 7*B* *versus* Fig. 6, *A*–*C*). Because the level of Not1 was reduced in *ccr4*Δ and *caf1*Δ mutant cells (Fig. 6*D*), it is likely that translation repression by tethered TNRC6 requires the integrity of CCR4-NOT complex. Next, we performed polysome analysis in *dhh1*Δ or *pat1*Δ mutant cells. Translation repression of *AUG-MS2* or *AUG-MS2-Rz* mRNAs by the Mid domain was abrogated in *dhh1*Δ or *pat1*Δ single mutants, as well as in the *dhh1*Δ*pat1*Δ double mutant (Fig. 7, *A*–E). These results indicate that both mRNA fate modulators are required for inhibition of translation by the tethered Mid domain of zebrafish TNRC6. To confirm the result of the polysome analysis, we performed pulse-labeling experiments to investigate whether Dhh1 and Pat1 are required for translation repression. Because N-terminally truncated MPT4 derived from *AUG-MS2* or *AUG-MS2-Rz* mRNAs contains no methionine (other than the initiator methionine) or cysteine, we used *GFP-MS2* and *GFP-MS2*-Rz mRNAs for the pulse-labeling experiments. The levels of synthesized GFP derived from reporter mRNAs were significantly reduced by tethered TNRC6A in the wild type (Fig. 1*I*), but translation repression was impaired in the *dhh1*Δ or *pat1*Δ single mutants and the *dhh1*Δ*pat1*Δ double mutant cells (Fig. 7*F*). These results demonstrate that the two mRNA fate modulators, Dhh1 and Pat1, not only facilitate mRNA decay from the 5′ end independently of translation and a poly(A) tail but also repress translation when the CCR4-NOT complex is recruited to mRNAs by the miRISC component TNRC6A.

DISCUSSION

In this study, we established a heterologous experimental system by tethering animal TNRC6 proteins to mRNAs in yeast. Polysome analysis, pulse-labeling experiments, and measurement of mRNA half-lives revealed that the tethered Mid domain fragment of zebrafish TNRC6A induces mRNA degradation and translation repression in yeast. This result strongly suggests that miRISC induces both translation repression and mRNA degradation via interactions with fundamental factors that are conserved across a wide range of eukaryotes. Indeed, the highly conserved proteins Dhh1 and Pat1 mediate these two functions through the CCR4-NOT complex, which is recruited by the Mid domain (Figs. 5 and 7). These two factors are involved in miRNA-mediated silencing in animals (11, 12, 25, 29, 33–35, 59), supporting the idea that TNRC6 can function in *S. cerevisiae* and suggesting that our system can be used to characterize the biologically relevant activities of miRISC. Although the data obtained in yeast with a truncated fragment of TNRC6 require careful validation in animal cells, the recapitulation of TNRC6-mediated silencing in yeast described here raises the possibility that genetic resources in yeast can be used to study basic principles of the miRNA system.

The Mid domain of TNRC6A interacted with the yeast CCR4-NOT complex via CIM1 and W-motifs within the Mid domain that mediate the same interactions in animals (Fig. 1*B*) (33, 34). This result, together with recent structural studies (11, 12), indicates that the conserved architecture of the CCR4-

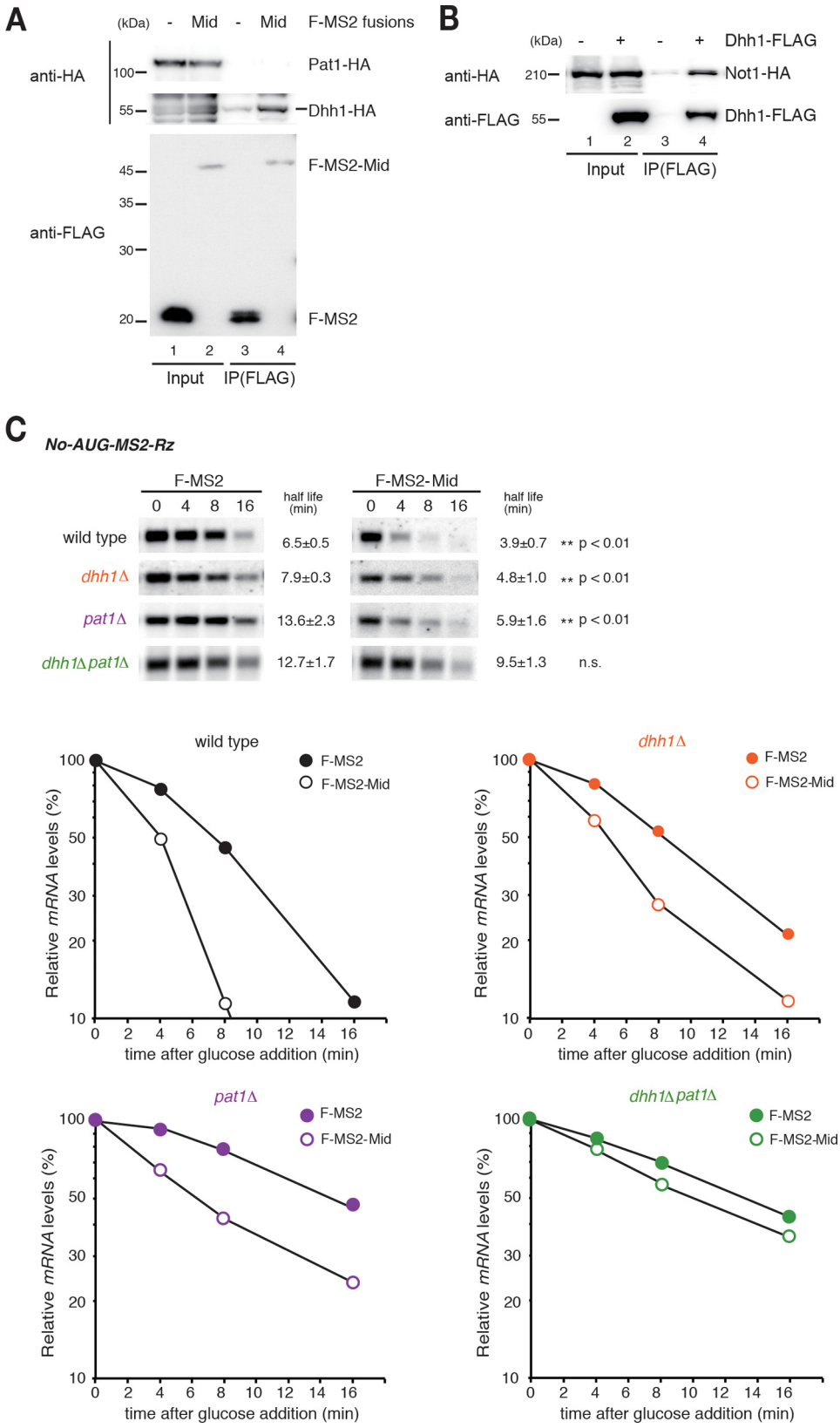

FIGURE 5. **mRNA decapping factors exert partially redundant functions in rapid mRNA decay from the 5′ end by tethered TNRC6A.** *A*, interaction of FLAG-MS2-Mid with yeast Dhh1-HA. Cell lysates of wild type cells transformed with the indicated plasmids were immunoprecipitated using anti-FLAG antibody. Total extract (*Input*) and immunoprecipitate (*IP*) were analyzed by Western blotting using anti-HA or anti-FLAG antibody. *B*, interaction of FLAG-Dhh1 with Not1-HA. Immunoprecipitation was performed as described in *A*. *C*, mRNA fate modulators Dhh1 and Pat1 have partially redundant functions in TNRC6AMid-mediated 5′-to-3′ mRNA decay independent of translation and a poly(A) tail. *Top*, Northern blotting analysis of *No-AUG-MS2-Rz* mRNA in the indicated cells. The half-lives of mRNA in the indicated cells are shown as the mean values of three independent experiments, with S.D. values. *Bottom*, graphs of the half-life analysis. The *p* value was calculated by using Student's *t* test.

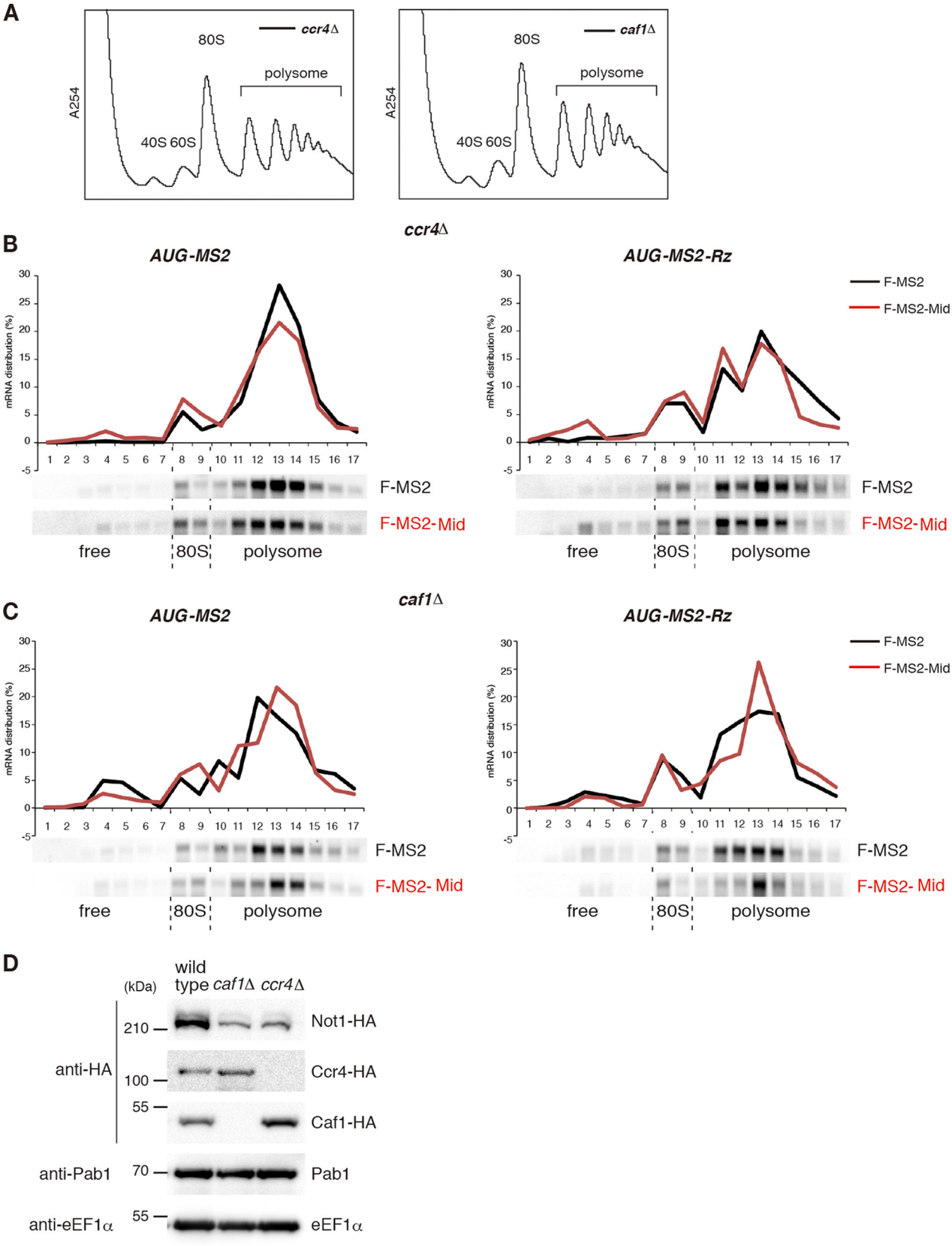

FIGURE 6. **The roles of CCR4-NOT complex in TNRC6A-mediated translation repression in yeast.** *A–C*, translation repression by tethered TNRC6A was almost diminished in *ccr4*Δ and *caf1*Δ mutant cells independent of a poly(A) tail. Cell extracts were prepared from indicated cells harboring the indicated plasmid, and polysome analysis was performed. RNA samples were analyzed by Northern blotting using a DIG-labeled *PGK1* 3′-UTR probe. *D*, the expression level of Not1 reduced in *caf1*Δ and *ccr4*Δ mutant cells. Endogenous *NOT1*, *CAF1*, and *CCR4* were tagged by 3× hemagglutinin (*HA*) in wild type, *caf1*Δ, and *ccr4*Δ mutant cells. Protein samples were analyzed by Western blotting using anti-HA, anti-Pab1 and anti-eEF1α antibodies.

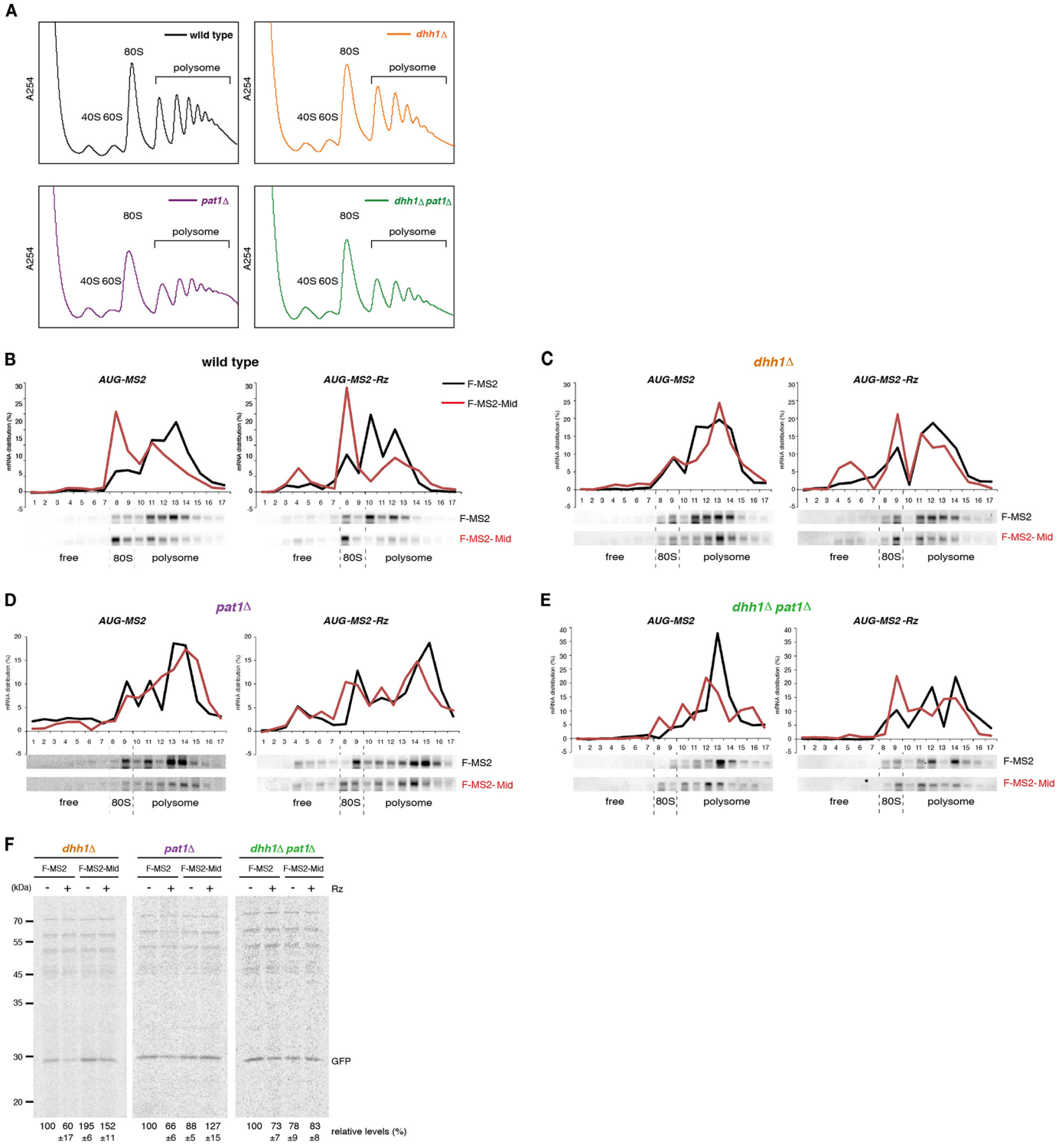

FIGURE 7. **The roles of decapping factors in TNRC6A-mediated translation repression in yeast.** *A–E*, cell extracts were prepared from wild type and the indicated mutant cells transformed with the indicated plasmids, and polysome analysis was performed. Distributions of the reporter RNAs were analyzed by Northern blotting. *F*, pulse-labeling experiments were performed using *dhh1*Δ, *pat1*Δ, and *dhh1*Δ*pat1*Δ mutant cells. GFP-MS2 and GFP-MS2-Rz protein levels reflect the mean values of three independent experiments, with S.D. values.

NOT complex provides a binding surface for GW182/TNRC6 proteins, thereby connecting miRISC to the mRNA fate modulators. Further biochemical and structural analysis in yeast will shed light on how this interaction evolved.

The interactions of GW182/TNRC6 proteins with PABP and CCR4-NOT deadenylase play crucial roles in both translational repression and degradation of miRNA targets (33–35, 37). mRNA degradation by miRNAs and GW182/TNRC6 requires both deadenylase and the DCP1-DCP2 decapping complexes (25, 60). In addition, GW182 recruits decapping enzymes to target mRNAs independently of deadenylation (38). In this study, we demonstrated that the tethered TNRC6A fragment

promoted decapping and 5′-to-3′ mRNA decay in a Not1-dependent but a poly(A) tail- and translation-independent manner (Figs. 2 and 3). The levels of decapped *No-AUG-MS2-Rz* mRNA were significantly increased in *xrn1*Δ cells expressing F-MS2-Mid (Fig. 3, *B* and *C*), indicating that the tethered Mid domain of TNRC6A recruits CCR4-NOT and the decapping complex and facilitates the decapping reaction independently of a poly(A) tail and translation. Together, these results suggest that mRNA decay caused by the Mid domain can mostly be attributed to the function of the yeast CCR4-NOT complex.

Our results indicate that GW182/TNRC6 stimulates mRNA decay in yeast in a decapping-dependent but poly(A) tail- and translation-independent manner. We also found that tethering of the TNRC6A Mid domain degraded m^7G-capped mRNA but not A-capped mRNA in zebrafish embryos (Fig. 4*D*). Moreover, miR-430 stimulated decapping and 5′-to-3′ degradation of *eif4ebp2* mRNA in zebrafish embryos even when the deadenylase activity of the CCR4-NOT complex was not fully ensured (Fig. 4, *F*, *G*, and *J*). These results imply that, at least for some mRNAs like *eif4ebp2*, miRISC promotes mRNA decay from the 5′ end by directly stimulating decapping before (or in parallel to) deadenylation. Although more comprehensive study with multiple transcripts in diverse animals is prerequisite to generalize this degradation mode of miRNAs, it is noteworthy that some mRNAs that are degraded in an Ago1-dependent manner are degraded when CAF1 is knocked down in *Drosophila* S2 cells (25). Conversely, not all Ago1-RISC target mRNAs strictly require mRNA fate modulators for their decay (29). These observations suggest that each mRNA is differentially susceptible to decapping and deadenylation during the process of miRNA-mediated degradation.

We found that rapid decay of *No-AUG-MS2-Rz* mRNA by the tethered TNRC6A Mid domain was abrogated in the *dhh1*Δ*pat1*Δ double mutant but not in the *dhh1*Δ or *pat1*Δ single mutants (Fig. 5). We propose that Dhh1 and Pat1 contribute to decapping via distinct pathways in the absence of translation and a poly(A) tail. In addition to inhibiting translation, Dhh1 and Pat1 may have redundant functions in the formation of the decapping complex. Consequently, in the *dhh1*Δ*pat1*Δ double mutant, the decapping complex may not be able to form, resulting in a very strong defect in decapping.

A prevailing view, based on *in vitro* experiments, is that miRNAs inhibit translation at the initiation step by an as yet unknown mechanism (39, 61–63). A recent study has suggested that miRNAs repress translation initiation in a manner dependent upon eIF4AII, which interacts with CNOT7 of the CCR4-NOT complex in mammalian cells (64). However, because eIF4AII is present neither in *Drosophila* nor in unicellular eukaryotes, such as *S. cerevisiae*, it remains to be determined how this factor affects translation initiation in general. In this study, we showed that the tethered Mid domain of TNRC6A repressed translation in yeast (Fig. 1, *G* and *H*; see also Fig. 7*B*). Hence, the repressive activity of TNRC6A recapitulated in yeast is independent of eIF4AII. In addition, others also observed that eIF4AII does not interact directly with CNOT1 MIF4G domain (11, 12, 43). Furthermore, recent *in vitro* studies showed that miRNAs trigger dissociation of eIF4A in *Drosophila* and both eIF4AI and eIF4AII in humans (65, 66). Apparently, more experiments will be necessary to determine the roles of eIF4AII in translation repression by miRNAs.

In cells expressing F-MS2-Mid protein, the levels of *GFP-MS2* or *AUG-MS2* mRNAs were reduced in the polysome fraction, but increased in the 80 S monosome and free fractions, relative to cells expressing the control MS2 protein (Figs. 1*G* and 7*B*). This effect was observed in a reporter mRNA lacking a poly(A) tail (Figs. 1*G* and 7*B*). These results suggest that the tethered Mid domain of TNRC6A may block the formation of 48 S preinitiation complex or inhibit the steps after 80 S formation by CCR4-NOT complex independently of a poly(A) tail.

How, then, does the CCR4-NOT complex inhibit translation? Polysome analysis and pulse-labeling experiments showed that translation repression by tethering of the Mid domain of TNRC6A was abrogated in *dhh1*Δ or *pat1*Δ single mutants as well as in the *dhh1*Δ*pat1*Δ double mutant (Fig. 7). Translationally repressed mRNAs in wild type cells contained a cap structure (Fig. 3, *D* and *E*). Moreover, stimulation of mRNA decay from the 5′ end was impaired only in the *dhh1*Δ*pat1*Δ double mutant, whereas translation repression by the tethered TNRC6A was suppressed in the *dhh1*Δ and *pat1*Δ single mutants (Fig. 7). These results clearly indicate that translation repression is not a consequence of decapping. The mRNA fate modulators Dhh1 and Pat1 independently repress translation *in vivo*, and they repress translation initiation *in vitro* by limiting the formation of a stable 48 S preinitiation complex (15). Notably, a human homolog of Dhh1, DDX6/RCK1/p54, interacts with miRISC and contributes to translation repression in cultured cells (11, 12, 43, 59), and GW182 associates with HPat in *Drosophila* cells (57). Our results in yeast therefore support the model in which the CCR4-NOT complex mediates translation repression, at least in part, via recruitment of mRNA fate modulators through a direct interaction with Dhh1. Further experiments will be necessary to determine the conserved roles of decapping factors Dhh1/DDX6/RCK1/p54 and Pat1/HPat/PatL1 in translation repression by GW182/TNRC6 as well as other CCR4-NOT-interacting proteins.

Acknowledgments—We thank Dr. Yukihide Tomari for the kind gift of a reagent and for helpful discussions. We also thank members of our laboratories for discussion and critical comments on the manuscript.

REFERENCES

1. Wahle, E., and Winkler, G. S. (2013) RNA decay machines: deadenylation by the Ccr4-not and Pan2-Pan3 complexes. *Biochim. Biophys. Acta.* **1829,** 561–570
2. Collart, M. A., and Panasenko, O. O. (2012) The Ccr4-Not complex. *Gene* **492,** 42–53
3. Miller, J. E., and Reese, J. C. (2012) Ccr4-Not complex: the control freak of eukaryotic cells. *Crit. Rev. Biochem. Mol. Biol.* **47,** 315–333
4. Basquin, J., Roudko, V. V., Rode, M., Basquin, C., Séraphin, B., and Conti, E. (2012) Architecture of the nuclease module of the yeast Ccr4-not complex: the Not1-Caf1-Ccr4 interaction. *Mol. Cell* **48,** 207–218
5. Petit, A. P., Wohlbold, L., Bawankar, P., Huntzinger, E., Schmidt, S., Izaurralde, E., and Weichenrieder, O. (2012) The structural basis for the interaction between the CAF1 nuclease and the NOT1 scaffold of the human CCR4-NOT deadenylase complex. *Nucleic Acids Res.* **40,** 11058–11072
6. Parker, R. (2012) RNA degradation in *Saccharomyces cerevisae*. *Genetics* **191,** 671–702
7. Coller, J., and Parker, R. (2004) Eukaryotic mRNA decapping. *Annu. Rev.*

Biochem. **73,** 861–890
8. Maillet, L., and Collart, M. A. (2002) Interaction between Not1p, a component of the Ccr4-not complex, a global regulator of transcription, and Dhh1p, a putative RNA helicase. *J. Biol. Chem.* **277,** 2835–2842
9. Ozgur, S., Chekulaeva, M., and Stoecklin, G. (2010) Human Pat1b connects deadenylation with mRNA decapping and controls the assembly of processing bodies. *Mol. Cell Biol.* **30,** 4308–4323
10. Haas, G., Braun, J. E., Igreja, C., Tritschler, F., Nishihara, T., and Izaurralde, E. (2010) HPat provides a link between deadenylation and decapping in metazoa. *J. Cell Biol.* **189,** 289–302
11. Mathys, H., Basquin, J., Ozgur, S., Czarnocki-Cieciura, M., Bonneau, F., Aartse, A., Dziembowski, A., Nowotny, M., Conti, E., and Filipowicz, W. (2014) Structural and biochemical insights to the role of the CCR4-NOT complex and DDX6 ATPase in microRNA repression. *Mol. Cell* **54,** 751–765
12. Chen, Y., Boland, A., Kuzuoğlu-Öztürk, D., Bawankar, P., Loh, B., Chang, C. T., Weichenrieder, O., and Izaurralde, E. (2014) A DDX6-CNOT1 complex and W-binding pockets in CNOT9 reveal direct links between miRNA target recognition and silencing. *Mol. Cell* **54,** 737–750
13. Tritschler, F., Braun, J. E., Motz, C., Igreja, C., Haas, G., Truffault, V., Izaurralde, E., and Weichenrieder, O. (2009) DCP1 forms asymmetric trimers to assemble into active mRNA decapping complexes in metazoa. *Proc. Natl. Acad. Sci. U.S.A.* **106,** 21591–21596
14. Tritschler, F., Eulalio, A., Helms, S., Schmidt, S., Coles, M., Weichenrieder, O., Izaurralde, E., and Truffault, V. (2008) Similar modes of interaction enable Trailer Hitch and EDC3 to associate with DCP1 and Me31B in distinct protein complexes. *Mol. Cell Biol.* **28,** 6695–6708
15. Coller, J., and Parker, R. (2005) General translational repression by activators of mRNA decapping. *Cell* **122,** 875–886
16. Minshall, N., Thom, G., and Standart, N. (2001) A conserved role of a DEAD box helicase in mRNA masking. *RNA* **7,** 1728–1742
17. Nakamura, A., Amikura, R., Hanyu, K., and Kobayashi, S. (2001) Me31B silences translation of oocyte-localizing RNAs through the formation of cytoplasmic RNP complex during *Drosophila* oogenesis. *Development* **128,** 3233–3242
18. Anderson, J. S., and Parker, R. (1996) RNA turnover: the helicase story unwinds. *Curr. Biol.* **6,** 780–782
19. Minshall, N., Kress, M., Weil, D., and Standart, N. (2009) Role of p54 RNA helicase activity and its C-terminal domain in translational repression, P-body localization and assembly. *Mol. Biol. Cell* **20,** 2464–2472
20. Fabian, M. R., Sonenberg, N., and Filipowicz, W. (2010) Regulation of mRNA translation and stability by microRNAs. *Annu. Rev. Biochem.* **79,** 351–379
21. Lim, L. P., Lau, N. C., Garrett-Engele, P., Grimson, A., Schelter, J. M., Castle, J., Bartel, D. P., Linsley, P. S., and Johnson, J. M. (2005) Microarray analysis shows that some microRNAs downregulate large numbers of target mRNAs. *Nature* **433,** 769–773
22. Giraldez, A. J., Mishima, Y., Rihel, J., Grocock, R. J., Van Dongen, S., Inoue, K., Enright, A. J., and Schier, A. F. (2006) Zebrafish MiR-430 promotes deadenylation and clearance of maternal mRNAs. *Science* **312,** 75–79
23. Mishima, Y., Giraldez, A. J., Takeda, Y., Fujiwara, T., Sakamoto, H., Schier, A. F., and Inoue, K. (2006) Differential regulation of germline mRNAs in soma and germ cells by zebrafish miR-430. *Curr. Biol.* **16,** 2135–2142
24. Wu, L., Fan, J., and Belasco, J. G. (2006) MicroRNAs direct rapid deadenylation of mRNA. *Proc. Natl. Acad. Sci. U.S.A.* **103,** 4034–4039
25. Behm-Ansmant, I., Rehwinkel, J., Doerks, T., Stark, A., Bork, P., and Izaurralde, E. (2006) mRNA degradation by miRNAs and GW182 requires both CCR4:NOT deadenylase and DCP1:DCP2 decapping complexes. *Genes Dev.* **20,** 1885–1898
26. Eulalio, A., Huntzinger, E., Nishihara, T., Rehwinkel, J., Fauser, M., and Izaurralde, E. (2009) Deadenylation is a widespread effect of miRNA regulation. *RNA* **15,** 21–32
27. Huntzinger, E., and Izaurralde, E. (2011) Gene silencing by microRNAs: contributions of translational repression and mRNA decay. *Nat. Rev. Genet.* **12,** 99–110
28. Rehwinkel, J., Behm-Ansmant, I., Gatfield, D., and Izaurralde, E. (2005) A crucial role for GW182 and the DCP1:DCP2 decapping complex in miRNA-mediated gene silencing. *RNA* **11,** 1640–1647
29. Eulalio, A., Rehwinkel, J., Stricker, M., Huntzinger, E., Yang, S. F., Doerks, T., Dorner, S., Bork, P., Boutros, M., and Izaurralde, E. (2007) Target-specific requirements for enhancers of decapping in miRNA-mediated gene silencing. *Genes Dev.* **21,** 2558–2570
30. Meister, G. (2013) Argonaute proteins: functional insights and emerging roles. *Nat. Rev. Genet* **14,** 447–459
31. Eulalio, A., Helms, S., Fritzsch, C., Fauser, M., and Izaurralde, E. (2009) A C-terminal silencing domain in GW182 is essential for miRNA function. *RNA* **15,** 1067–1077
32. Till, S., Lejeune, E., Thermann, R., Bortfeld, M., Hothorn, M., Enderle, D., Heinrich, C., Hentze, M. W., and Ladurner, A. G. (2007) A conserved motif in Argonaute-interacting proteins mediates functional interactions through the Argonaute PIWI domain. *Nat. Struct. Mol. Biol.* **14,** 897–903
33. Fabian, M. R., Cieplak, M. K., Frank, F., Morita, M., Green, J., Srikumar, T., Nagar, B., Yamamoto, T., Raught, B., Duchaine, T. F., and Sonenberg, N. (2011) miRNA-mediated deadenylation is orchestrated by GW182 through two conserved motifs that interact with CCR4-NOT. *Nat. Struct. Mol. Biol.* **18,** 1211–1217
34. Chekulaeva, M., Mathys, H., Zipprich, J. T., Attig, J., Colic, M., Parker, R., and Filipowicz, W. (2011) miRNA repression involves GW182-mediated recruitment of CCR4-NOT through conserved W-containing motifs. *Nat. Struct. Mol. Biol.* **18,** 1218–1226
35. Braun, J. E., Huntzinger, E., Fauser, M., and Izaurralde, E. (2011) GW182 proteins directly recruit cytoplasmic deadenylase complexes to miRNA targets. *Mol. Cell* **44,** 120–133
36. Christie, M., Boland, A., Huntzinger, E., Weichenrieder, O., and Izaurralde, E. (2013) Structure of the PAN3 pseudokinase reveals the basis for interactions with the PAN2 deadenylase and the GW182 proteins. *Mol. Cell* **51,** 360–373
37. Fabian, M. R., Mathonnet, G., Sundermeier, T., Mathys, H., Zipprich, J. T., Svitkin, Y. V., Rivas, F., Jinek, M., Wohlschlegel, J., Doudna, J. A., Chen, C. Y., Shyu, A. B., Yates, J. R., 3rd, Hannon, G. J., Filipowicz, W., Duchaine, T. F., and Sonenberg, N. (2009) Mammalian miRNA RISC recruits CAF1 and PABP to affect PABP-dependent deadenylation. *Mol. Cell* **35,** 868–880
38. Nishihara, T., Zekri, L., Braun, J. E., and Izaurralde, E. (2013) miRISC recruits decapping factors to miRNA targets to enhance their degradation. *Nucleic Acids Res.* **41,** 8692–8705
39. Fukaya, T., and Tomari, Y. (2012) MicroRNAs mediate gene silencing via multiple different pathways in drosophila. *Mol. Cell* **48,** 825–836
40. Mishima, Y., Fukao, A., Kishimoto, T., Sakamoto, H., Fujiwara, T., and Inoue, K. (2012) Translational inhibition by deadenylation-independent mechanisms is central to microRNA-mediated silencing in zebrafish. *Proc. Natl. Acad. Sci. U.S.A.* **109,** 1104–1109
41. Fukaya, T., and Tomari, Y. (2011) PABP is not essential for microRNA-mediated translational repression and deadenylation in vitro. *EMBO. J.* **30,** 4998–5009
42. Bawankar, P., Loh, B., Wohlbold, L., Schmidt, S., and Izaurralde, E. (2013) NOT10 and C2orf29/NOT11 form a conserved module of the CCR4-NOT complex that docks onto the NOT1 N-terminal domain. *RNA. Biol.* **10,** 228–244
43. Rouya, C., Siddiqui, N., Morita, M., Duchaine, T. F., Fabian, M. R., and Sonenberg, N. (2014) Human DDX6 effects miRNA-mediated gene silencing via direct binding to CNOT1. *RNA* **20,** 1398–1409
44. Goldstrohm, A. C., Seay, D. J., Hook, B. A., and Wickens, M. (2007) PUF protein-mediated deadenylation is catalyzed by Ccr4p. *J. Biol. Chem.* **282,** 109–114
45. Goldstrohm, A. C., Hook, B. A., Seay, D. J., and Wickens, M. (2006) PUF proteins bind Pop2p to regulate messenger RNAs. *Nat. Struct. Mol. Biol.* **13,** 533–539
46. Drinnenberg, I. A., Weinberg, D. E., Xie, K. T., Mower, J. P., Wolfe, K. H., Fink, G. R., and Bartel, D. P. (2009) RNAi in budding yeast. *Science* **326,** 544–550
47. Suk, K., Choi, J., Suzuki, Y., Ozturk, S. B., Mellor, J. C., Wong, K. H., MacKay, J. L., Gregory, R. I., and Roth, F. P. (2011) Reconstitution of human RNA interference in budding yeast. *Nucleic Acids Res.* **39,** e43
48. Inada, T., and Aiba, H. (2005) Translation of aberrant mRNAs lacking a termination codon or with a shortened 3′-UTR is repressed after initiation

in yeast. *EMBO J.* **24,** 1584–1595
49. Tsuboi, T., and Inada, T. (2010) Tethering of poly(A)-binding protein interferes with non-translated mRNA decay from the 5′ end in yeast. *J. Biol. Chem.* **285,** 33589–33601
50. Mumberg, D., Müller, R., and Funk, M. (1994) Regulatable promoters of *Saccharomyces cerevisiae*: comparison of transcriptional activity and their use for heterologous expression. *Nucleic Acids Res.* **22,** 5767–5768
51. Chekulaeva, M., Filipowicz, W., and Parker, R. (2009) Multiple independent domains of dGW182 function in miRNA-mediated repression in *Drosophila*. *RNA* **15,** 794–803
52. Bazzini, A. A., Lee, M. T., and Giraldez, A. J. (2012) Ribosome profiling shows that miR-430 reduces translation before causing mRNA decay in zebrafish. *Science* **336,** 233–237
53. Rissland, O. S., and Norbury, C. J. (2009) Decapping is preceded by 3′ uridylation in a novel pathway of bulk mRNA turnover. *Nat. Struct. Mol. Biol.* **16,** 616–623
54. Braun, J. E., Truffault, V., Boland, A., Huntzinger, E., Chang, C. T., Haas, G., Weichenrieder, O., Coles, M., and Izaurralde, E. (2012) A direct interaction between DCP1 and XRN1 couples mRNA decapping to 5′ exonucleolytic degradation. *Nat. Struct. Mol. Biol.* **19,** 1324–1331
55. Aanes, H., Winata, C. L., Lin, C. H., Chen, J. P., Srinivasan, K. G., Lee, S. G., Lim, A. Y., Hajan, H. S., Collas, P., Bourque, G., Gong, Z., Korzh, V., Aleström, P., and Mathavan, S. (2011) Zebrafish mRNA sequencing deciphers novelties in transcriptome dynamics during maternal to zygotic transition. *Genome Res.* **21,** 1328–1338
56. van Dijk, E., Cougot, N., Meyer, S., Babajko, S., Wahle, E., and Séraphin, B. (2002) Human Dcp2: a catalytically active mRNA decapping enzyme located in specific cytoplasmic structures. *EMBO. J.* **21,** 6915–6924
57. Jäger, E., and Dorner, S. (2010) The decapping activator HPat a novel factor co-purifying with GW182 from *Drosophila* cells. *RNA Biol.* **7,** 381–385
58. Barišić-Jäger, E., Krecioch, I., Hosiner, S., Antic, S., and Dorner, S. (2013) HPat a decapping activator interacting with the miRNA effector complex. *PLoS One* **8,** e71860
59. Chu, C. Y., and Rana, T. M. (2006) Translation repression in human cells by microRNA-induced gene silencing requires RCK/p54. *PLoS Biol.* **4,** e210
60. Chen, C. Y., Zheng, D., Xia, Z., and Shyu, A. B. (2009) Ago-TNRC6 triggers microRNA-mediated decay by promoting two deadenylation steps. *Nat. Struct. Mol. Biol.* **16,** 1160–1166
61. Zdanowicz, A., Thermann, R., Kowalska, J., Jemielity, J., Duncan, K., Preiss, T., Darzynkiewicz, E., and Hentze, M. W. (2009) *Drosophila* miR2 primarily targets the m7GpppN cap structure for translational repression. *Mol. Cell* **35,** 881–888
62. Thermann, R., and Hentze, M. W. (2007) Drosophila miR2 induces pseudo-polysomes and inhibits translation initiation. *Nature* **447,** 875–878
63. Mathonnet, G., Fabian, M. R., Svitkin, Y. V., Parsyan, A., Huck, L., Murata, T., Biffo, S., Merrick, W. C., Darzynkiewicz, E., Pillai, R. S., Filipowicz, W., Duchaine, T. F., and Sonenberg, N. (2007) MicroRNA inhibition of translation initiation *in vitro* by targeting the cap-binding complex eIF4F. *Science* **317,** 1764–1767
64. Meijer, H. A., Kong, Y. W., Lu, W. T., Wilczynska, A., Spriggs, R. V., Robinson, S. W., Godfrey, J. D., Willis, A. E., and Bushell, M. (2013) Translational repression and eIF4A2 activity are critical for microRNA-mediated gene regulation. *Science* **340,** 82–85
65. Fukao, A., Mishima, Y., Takizawa, N., Oka, S., Imataka, H., Pelletier, J., Sonenberg, N., Thoma, C., and Fujiwara, T. (2014) MicroRNAs trigger dissociation of eIF4AI and eIF4AII from target mRNAs in humans. *Mol. Cell* **56,** 79–89
66. Fukaya, T., Iwakawa, H. O., and Tomari, Y. (2014) MicroRNAs block assembly of eIF4F translation initiation complex in *Drosophila*. *Mol. Cell* **56,** 67–78
67. Kuroha, K., Tatematsu, T., and Inada, T. (2009) Upf1 stimulates degradation of the product derived from aberrant messenger RNA containing a specific nonsense mutation by the proteasome. *EMBO Rep.* **10,** 1265–1271